Bachelor Thesis

Stockholm University

Degree Project in
Geochemistry 30 hp

Inverse calibration of lake surface gas concentration

Four years of diffusive methane release from a small subarctic lake

Kristian Andersson

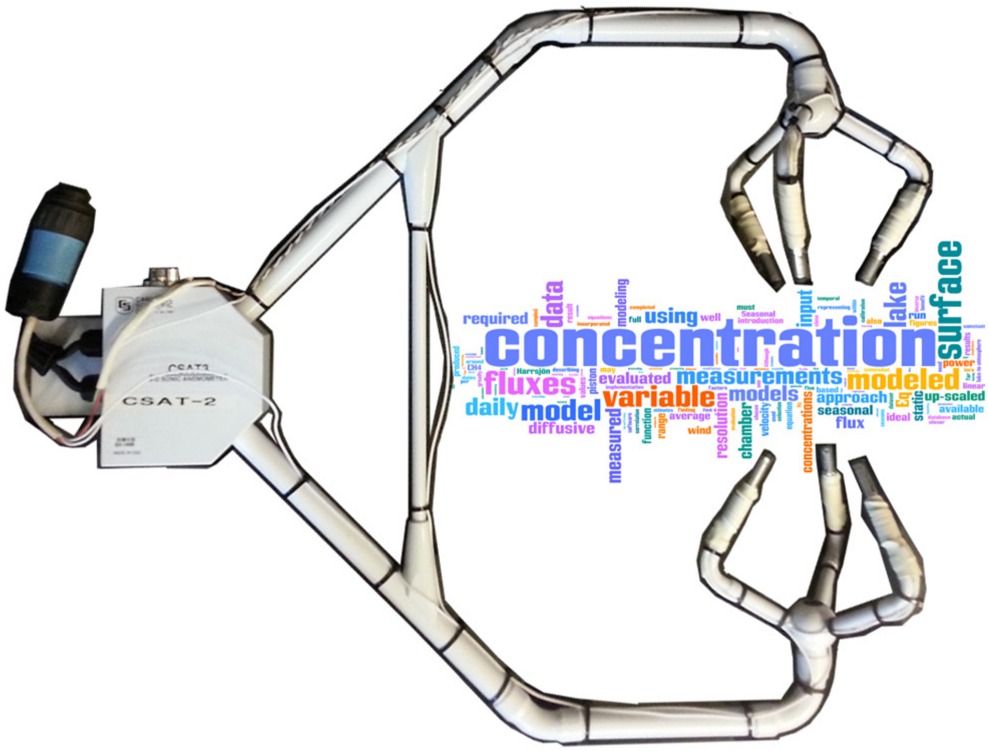

Stockholm 2015

Department of Geological Sciences
Stockholm University
SE-106 91 Stockholm

1 Abstract

With methane considered a major player among the greenhouse gases comes the need for reliable quantification of atmospheric methane sources. In oxygen poor sediment of lakes, decomposition of organic material result production of methane. Release occurs both as bubbles (ebullition) and in the form of diffusive transfer across the lake-atmosphere interface. In this paper, using five piston velocity models, the diffusive gas flux from a subarctic lake was calculated at temporal scales ranging from one minute up to an entire ice-free season (120 days). Modeled results were compared to field observations with the intent of finding the combination of model and temporal resolution producing results closest matching those measured.

Simplified, the main drivers of the diffusive gas flux are wind speed and lake surface gas concentration. With concentration only given as a fairly broad range for this lake, initial modeling efforts were performed assuming static lake surface concentration (range average). Resulting fluxes from these model runs ended up several factors larger than those measured at lake.

Based on the assumption that high wind might affect the surface concentration of the (shallow) lake, a variable concentration approach was established. On the 40 dates with actual flux measurements available, the models were ran in an inverse fashion; instead of resulting in a flux, results now indicated the surface concentration that would have been required for the modeled fluxes to meet the measured fluxes. Per model, these required (or ideal) surface concentration figures where plotted as function of daily U_{10} (wind at 10 m height) and linear equations describing the correlation were used as wind-dependent *variable concentration* in subsequent runs. Results following the introduction of variable (or calibrated) surface concentration significantly improved performance of all models. Using input data in daily resolution and the variable concentration approach, fluxes calculated from the *power function* by Cole and Caraco (1998) were 91% of the up-scaled measured fluxes for season 2010, 112% for season 2011, and 102% for season 2012, the latter being the best model-observation agreement obtained. These results suggest an improved method for applying wind-based models of gas transfer flux to small lakes, where surface renewal rates may be lake-dependent, and not fully described by the wind-speed models alone.

2 Index

4 Introduction

Methane (CH_4) is part of a greenhouse gas trio, the two other being carbon dioxide (CO_2) and nitrous oxide (N_2O), responsible for 80% of the total radiative forcing from *well-mixed* greenhouse gases (Ciais et al., 2013). The well-mixed keyword relates to the nearly homogeneous distribution (concentration) of these gases throughout the troposphere. For comparison, tropospheric concentrations of the “Chief among the greenhouse gases”, as Sun and Lindzen (1993) chose to call water vapor, vary greatly both horizontally and vertically.

Of total CH_4 emissions, the anthropogenic contribution is estimated at 50 to 65%. Compared to preindustrial figures, the 2011 atmospheric CH_4 concentration of 1803 ppb translates to a 150% increase. For the time period covered by ice-cores (800 000 years) this is an all-time high (Ciais et al., 2013). Although concentrations of atmospheric CH_4 stabilized in the late 1990s, measurements from 2007 and onwards tell of renewed increase in concentrations (Ciais et al., 2013). Table 1 lists the CH_4 budget for time period 2000 to 2009 as described by the Intergovernmental Panel on Climate Change (IPCC) (Ciais et al., 2013).

Lakes and wetlands, where anoxic decomposition of organic material results in production of CH_4, are among the natural sources for atmospheric CH_4. Considering that the IPCC states that *“there is medium confidence that emissions of CH_4 from wetlands are likely to increase under elevated CO_2 and a warmer climate”* and *“there is low confidence in quantitative projections of these projections”* (Ciais et al., 2013), along with the amplified effects of global warming exhibited in the arctic (Jeffries, 2014), it is no surprise that these inland waters (possibly changing) role in the global carbon cycle have come an area of study (Tranvik, 2009).

CH_4 produced in lake sediment enters the atmosphere by diffusion and ebullition. The diffusive flux from liquid to gas, topic of this study, phase can be illustrated using the two-layer film approach in Fig. 1 as described by Liss and Slater (1974). In the model, the two main bodies (the gas phase C_g and the liquid phase C_l) are assumed well-mixed. The phase-separating interface is illustrated as two films. Applying Fick’s first law to the two-layer system allows for surface-to-air diffusive flux calculation (Liss and Slater, 1974; Cole et al., 2010). With known (measured) air-equilibrium and water surface gas concentrations the resulting diffusive flux is only depending on the piston velocity (k), often conceptualized as the height of water pillar reaching the interface per unit time. In its most trivial form, calculation of k only depends on a small set of readily measurable meteorological parameters such as wind speed and water temperature.

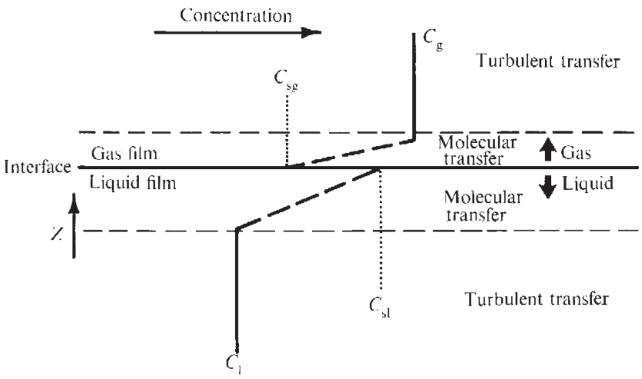

Figure 1. Two layer model of sea to air interface (Liss and Slater, 1974).

Quantification of diffusive CH_4 fluxes from subarctic lakes derived from readily measureable meteorological parameters should be of great value for any attempt at including such fluxes, or their possible feedback, into the global climate model. In this paper, meteorological data collected at, and around, a small subarctic lake (Inre Harrsjön) surrounded by wetland is applied to (some of the) existing models for evaluation of diffusive lake-to-atmosphere gas fluxes. Full season fluxes were modeled for the ice-free (roughly) periods of 2009, 2010, 2011 and 2012. Besides full season fluxes models were also ran using finer temporal resolutions, however, lack of input data constrained the fine resolution modeling to only cover two seven day intervals, one in August 2010 and the other in July 2011. From comparison of model result and on-site measurements understanding can be gained regarding which, if any, of the models that best describe the diffusive flux from the lake.

Table 1. CH_4 budget for years 2000 through 2009 based on figures from the IPCC (Ciais et al., 2013).

Source	**2000 – 2009 CH_4 Flux (Tg y^{-1})**			**Percent of total (Based on average)**
	Min	**Max**	**Avg**	
Wetlands	177	184	180.5	28
Agriculture and Waste	187	224	205.5	32
Fossil fuel	85	105	95	15
Other natural sources (including fresh water emissions)	61	200	130.5	20
Biomass and biofuel burning	32	39	35.5	6

5 Study site

Inre Harrsjön (68°21'29.9"N, 19°02'46.7"E) (Fig. 2), a small (0.02 km^2) and shallow lake with volume of 38300 m^3, was the object of this study. The lake belongs to the Stordalen Mire complex (68°21′36′′N, 19°03′02′′E) east of Abisko, northern Sweden. From a permafrost perspective, this subarctic region of Sweden resides in the discontinuous permafrost zone (Karlsson et al., 2010). Although not being of thermokarst origin, the lake is considered representative of the typical shallow subarctic lake (Wik et al., 2014).

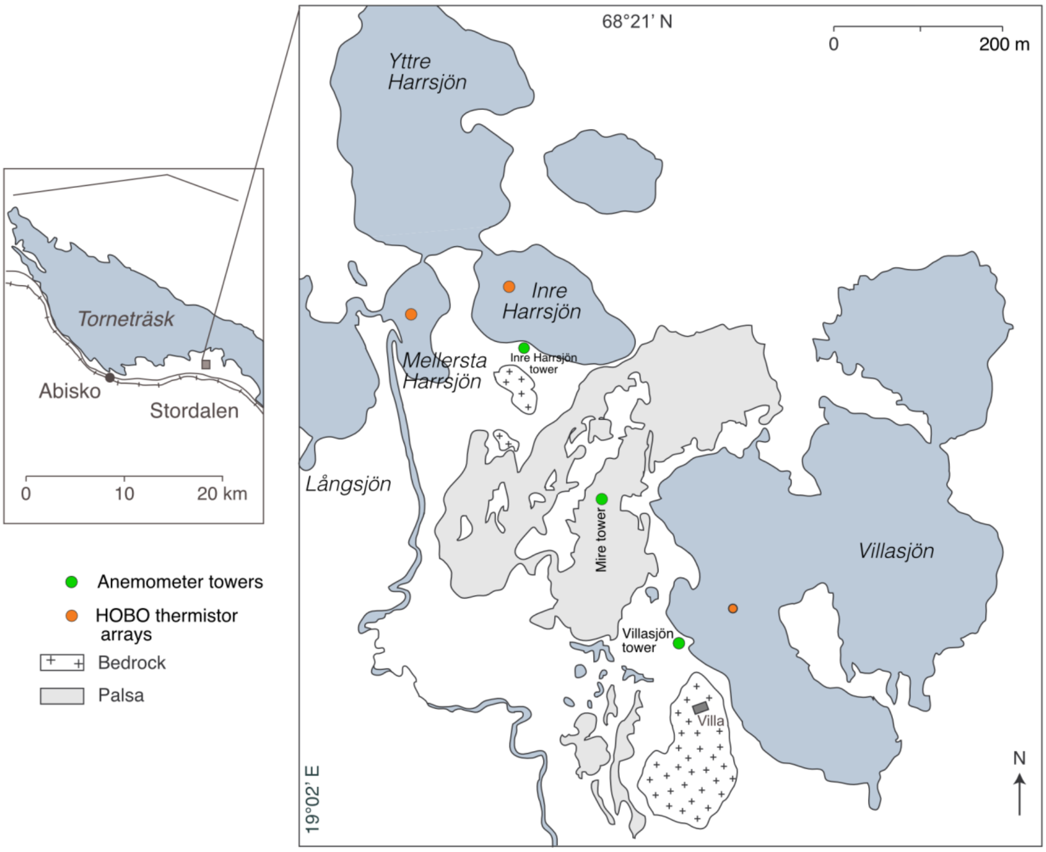

Figure 2. Inre Harrsjön is located within the Stordalen mire complex, northern Sweden. Approximate position of anemometer towers marked in green. Figure adapted from Wik et al. (2014).

From the result of a statistical analysis of climate data collected by Abisko Scientific Research Station (ANS) since the early 20th century Callaghan et al. (2010) describe this region as not only subjected to dramatic changes in climate, but also increasing rates of change. Both winter and summer temperatures are increasing, effectively raising mean annual temperature above the 0°C threshold (Callaghan et al. 2010). Also, permafrost is disappearing or exhibiting increasing depth of active layer (Callaghan et al. 2010). In another study of the mire complex, thawing permafrost and changes in vegetation are associated to an increase of landscape-scale CH_4 emissions, all likely caused by elevated temperatures (Christensen et al., 2004). With the perspective of this study, the hotter seasons and the diminishing permafrost could lead to greater load of total organic carbon reaching the lake, thus enabling an increase of the CH_4 produced. Previous studies have suggested strong correlation between lake sediment temperature and production of CH_4, with higher sediment temperature resulting in increased microbial activity hence increased CH_4 production (Wik et al., 2013; Wik et al. 2014).

6 Data and data sampling

Generally, the source datasets used throughout this exercise are vast, and in total they span millions of rows making any inclusion in the report impossible.

6.1 Wind

6.1.1 Inre Harrsjön Lake Tower

Wind speed and direction measurements stem from two tower-mounted Campbell Scientific, Logan, Utah, USA, CSAT3 3D high frequency sonic anemometers. The tower was positioned at the lake's shore; see Fig. 2 for approximate position. Sonic anemometers were mounted 115 cm and 205 cm above water surface. Throughout this exercise the sonic anemometers were referred to as fast2 and fast3, with fast3 mounted above fast2. Lake tower high frequency wind data was used in the search of best-fitting *k*-model for temporal resolutions spanning from one minute to seven days. Initially the measurements from these two high frequency sonic anemometers were to be used in turbulence based flux modeling, such as by MacIntyre et al. (2010). Limited availability in the high frequency dataset however led to the turbulence approach being abandoned in favor of other models. Friction velocity (u*) figures calculated from the high frequency data, using covariance equations described by Aubinet et al. (2012), is presented Appendix B (Fig. B-1 through B-4).

6.1.2 Villasjön Shore Lake Tower

The Villasjön Shore Lake tower was located on the southern shore of Villasjön, about 400 m southwest of the Inre Harrsjön tower. Wind data measured at 30 minutes resolution served input to the final long-term flux calculations for year 2012. Measurements were produced using a 3D sonic anemometer (Gill R3-50 manufactured by Gill Instruments Limited, Hampshire, UK). In calculation of U_{10} original measuring height of 2.92 m was assumed. Villasjön shore lake tower data is courtesy of Mathilde Jammet and Thomas Friborg, Copenhagen University. Approximate position marked in Fig. 2.

6.1.3 Mire Tower

30-minutes resolution wind measured at the mire separating the two lakes served input to the long-term flux calculations for years 2009, 2010 and 2011. In conversion to U_{10}, measuring height of 2 m was assumed. Mire tower data is courtesy of Nigel Roulet and Silvie Harder, McGill University. Approximate position marked in Fig. 2.

6.2 Water temperature

Water temperature data for depths 10, 30, 50, 100, 300 and 500 cm logged at five-minute intervals using several HOBO Water Temperature Pro v2 Data Logger (U22-001) manufactured by Onset Computer Corporation, Bourne, Massachusetts, USA, served as input in calculation of Schmidt number (section 8.2). Again, the dataset is vast and therefore not included with this document.

6.3 Measured CH_4 fluxes and concentrations

CH_4 flux, both as ebullition and diffusion, from Inre Harrsjön has been studied in detail using chamber techniques. The diffusive flux, target of this study, has been measured using shielded chambers. Table A-1 in appendix A lists all such chamber measurements available for this report. Knowing the surface and air-equilibrium concentrations of CH_4 allows for calculation of diffusive flux from model k-values, enabling comparison to actual measured fluxes. From unpublished data (Crill, 2014) the water surface concentrations is said to range from 0.3 to 2 µmol L^{-1}. Air-equilibrium concentration, again unpublished data (Crill, 2014), was considered fixed at 3.5 nmol $L^{-1.}$ Unit conversions assumed CH_4 molar weight of 16.0425 g mol^{-1}.

6.4 Flux capacity

At a late stage in the modeling exercise the thought struck that perhaps the piston velocities calculated might be high enough to have a degassing effect on actual lake CH_4 concentrations. Fig. 2 shows a lake of which the depth on a large portion is no greater than 2 meters. If this "thought experiment" lake would be 2 meters deep all around, fully mixed and experience no recharge of CH_4 from its sediment then a piston velocity of 20 cm h^{-1} would effectively deplete all CH_4 from the water in 10 hours. The real lake obviously doesn't mimic this thought lake, sediment to water flux does occur and diffusive lake-to-atmosphere flux decreases with dropping surface concentration. However, the magnitude of fluxes across this sediment-to-lake interface (which really is out of scope for this paper) should be of interest when comparing the modeled result to the measured. Huttunen et al. (2006) evaluated sediment to lake fluxes for eight boreal lakes located in Finland. For the two northernmost lakes in the study, Porttipahta (68°03′N, 26°41′E) and Lokka (67°57′N, 26°41′E) the warm period sediment to lake CH_4 fluxes were estimated to 25.4 mg m^{-2} d^{-1} and 0.44 mg m^{-2} d^{-1}, respectively (Huttunen et al., 2006). Sediment to water flux in Lake Lokka was by far the lowest of the lakes studied, a fact that indicate sediment produced CH_4 being released through ebullitive transport instead of diffusion (Huttunen et al., 2006).

7 Processing available data

The sheer amount of data available for this modeling exercise ruled out any chance of manually performing the required calculations. Instead it was opted for the creation of a database that would hold all available data. Along with the database, proper interfaces for reading and writing to it was created. (Author's) previous knowledge of MySQL database engine and Java programming language led to the choice of using MySQL 5.6.15 database engine for storage, and NetBeans IDE 7.4 for implementation (programing) of read/write interfaces and modeling logic. Java modeling result was output in comma-separated text to enable easy import to Microsoft Excel for final evaluation.

7.1 Source formats

Data used throughout this exercise were delivered in various formats. High frequency wind (along with several other meteorological parameters) data from the Inre Harrsjön tower were given in binary file format as produced by CR3000 and CR1000 microloggers manufactured by Campbell Scientific, Logan, Utah, USA. Water temperature was available in Microsoft Excel file format. Diffusive flux measurements were also given in Microsoft Excel format. Meteorological data from ANS were also incorporated in the projects database, however result obtained using this data was chosen not to be included in the report. The data from ANS was originally available in plain text files. Wind data from the mire tower were read from Microsoft Excel and finally, the wind data measured by the Villasjön shore lake tower were originally available in plain text files.

7.2 Source data conversion and verification

Micrologger binary files were converted to plain text using Campbell Scientific Card Convert 1.6. Water temperature source files were checked for format consistency, and altered when required, a procedure that was repeated for the data from ANS.

7.3 Database loading

Custom software for reading and verifying the content of the different files types, as well as writing the values to database, were implemented in Java programming language using previously mentioned NetBeans IDE 7.4 software. Only a subset of the parameters available in the source data was used during model runs, however all measured variables made it to the database thus are available for possible future work.

7.4 Extra database fields

Inre Harrsjön tower horizontal wind data was originally supplied in separate X and Y vectors. To avoid repetitive conversion of the horizontal wind vectors two fields, representing horizontal wind direction and speed, were added to the database. These fields for horizontal wind speed and direction were populated by the result achieved from running X and Y vector values through a function based around Java atan2 method, all in accordance with the CSAT-3 3D sonic anemometer manual (Campbell Scientific, 2014). The Inre Harrsjön tower azimuth was taken into consideration in calculation of the horizontal wind speed and direction. After the (somewhat long running) database update operation for population of the two fields, horizontal wind data (as now stored) was ready to use without further modification. Original X and Y vector values were kept in the database.

7.5 Data retrieval and interpolation

With the data loaded into the database, methods for data retrieval was programmed as required. Actual k_{600} models (see chapter 8) were implemented in Java. The final solution fit the description of a multi-tier model where database, logic and presentation reside separate from each other, i.e. the logic layer never look directly into the database, instead it will ask the database tier to supply whatever data required. This methodology, when implemented correctly, ensure that code (method calls) is reused throughout the entire application and if e.g. a database field is added then this change will only effect the database tier. As comparison, if change would be performed to the structure of the underlying database and the logic and/or presentation would talk directly to the database, then such change would have to be reflected in each and every call made from the logic/presentation tier. The multi-tier approach also allows further logic (e.g. another piston velocity model) to be included without having to write any database related code. Currently the only presentation (output) of result from the software is as comma-separated text. This could well be extended to present resulting data in any format or for any client (e.g. web browser, Microsoft Excel). Report generating was implemented so that data can be calculated for any date interval using (theoretically) any temporal resolution.

7.6 Database - summary

Data types used in database were selected to match source data type. Floating numbers were stored with MySQL decimal data type allowing nine decimal positions. Currently, the database consists of 19 tables. Row count, summarized across all tables, exceeded 284 million with a total number of measurements (considering that each row holds several measurements) just above six billion. Unfortunately, a large portion of the data set is unusable due to erratic performance of the sonic anemometers on the Inre Harrsjön tower.

8 Models and Methods

8.1 Modeling and temporal resolution

Having input wind data of high resolution (20 Hz) as well as data with coarser sampling resolution (30 minutes) allowed for model evaluation at several temporal scales.

8.1.1 High frequency evaluation

Using wind data measured at 20 Hz, results for all (piston velocity) models considered throughout this report results were calculated for 1, 5, 10, 30, 60 and 1440 minutes. The results from modeling were compared to the measured diffusive CH_4 flux data with the intent of finding the model that best represent the measured fluxes, as well as the temporal resolution at which the model performs at its best.

An initial analysis of the high frequency wind data showed that, although the logging equipment had been running, there were several (large) gaps where no valid measurements had been recorded. Eventually two seven-day spans with no, or less than 1%, missing records of measured wind data were identified. These two intervals, August 4th to August 10th 2010 and July 22nd to July 29th, were used in the high frequency model evaluation.

8.1.2 Seasonal average evaluation

In addition to running the models using high frequency wind input, seasonal averages from two sets of half hourly wind data were used with the piston velocity models to estimate diffusive CH_4 flux in a seasonal perspective. Seasonal fluxes were calculated based on daily averages as well as on full season input averages.

8.2 Gas Exchange Model

Although gas exchange between water surfaces and atmosphere rely on complex relations and variations in climate parameters the process allows for description through the simplified two-layer system in Fig. 1 (Liss and Slater, 1974). Applying Fick's first law to the two-layer system allows for diffusive flux calculation using Eq. (1)(Liss and Slater, 1974; Cole et al., 2010).

$$F = k(C_{sur} - C_{eq}) \quad (1)$$

where F is the diffusive flux in mg m^{-2} d^{-1}, k is the piston velocity (gas exchange constant, see separate section 8.3) in m d^{-1}, C_{sur} is surface water concentration in mg m^{-3} and C_{eq} is the air-equilibrium concentration in mg m^{-3}.

8.3 Piston Velocity

Unlike wind, temperature and concentration parameters, there is no way to measure the piston velocity. As stated by Cole et al. (2010) the piston velocity can be conceptualized as the water column height equilibrating with the atmosphere over time; a process related to the (turbulent) energy exchange across the air-water interface. Relating back to Fig. 1, the interface (the two film concept) separating the liquid and gas bodies restricts the gas flow. Energy input, increase in turbulence, at the interface weaken the resistance. In all models evaluated, wind speed at 10 (U_{10}) act main driver for turbulence. It should however be noted that the turbulence at the surface doesn't depend on wind alone. MacIntyre et al. (2010) used a far more complex *surface renewal model* based on e.g. net heat flux, buoyancy flux and lake active mixing layer thickness among other parameters to appreciate gas transfer coefficient. The model was originally considered for this evaluation; however lack of precision in water temperature measurements would render results useless. Also, piston velocity for a specific gas depends on kinematic viscosity of water qualities (temperature and salinity) and diffusion coefficient of the gas.

The models for evaluation of piston velocity used throughout this study all report the piston velocity as k_{600} which translate to piston velocity normalized for CO_2 in freshwater at 20°C, i.e. result from models would be correct if the gas in question was CO_2 and lake surface temperature was 20°C (Wanninkhof, 1992). Eq. 2 details the relationship between piston velocity coefficients for different gases, allowing calculation of $k_{any\text{-}gas\ any\ temperature}$ (Guérin et al., 2007).

$$k_{g,T} = k_{600}(600/Sc_{g,T})^n \quad (2)$$

where $k_{g,T}$ is piston velocity for given gas-temperature combination, k_{600} is piston velocity for gas with Schmidt number 600 (CO_2 at 20°C, freshwater), $Sc_{g,T}$ is Schmidt number for given gas-temperature combination and the n exponent is related to the turbulence at water surface. Further following Guérin et al. (2007) two values were used for n in this study; 2/3 for $U_{10} < 3.7$ ms^{-1} and 0.5 for all other U_{10}.

To estimate the total diffusive flux of CH_4 from the lake the resulting k_{600} figures needed to be converted to k for CH_4 at period-average surface temperature. Following Wanninkhof (1992) Schmidt number was calculated using Eq. (3).

$$Sc_{g,T} = A - BT + CT^2 - DT^3 \quad (3)$$

where $Sc_{g,T}$ is Schmidt number for given gas at water surface temperature T (°C) and A through D are gas specific coefficients.
With gas being CH_4 and temperatures ranging from 0 to 30°C the Schmidt number was calculated using (4) (Wanninkhof, 1992).

$$Sc_{CH4,T} = 1897.8 - 114.28T + 3.2902T^2 - 0.039061T^3 \quad (4)$$

Water temperature measured at 10 cm depth was considered representative of water surface temperature. For a given temporal resolution, the average of all available 10 cm temperature data within the time period was used in calculation of the Schmidt number. For one-minute intervals, average of the closest pre and post timestamp measurements were used. Water temperature data wasn't complete and where no temperature data could be located for a timestamp the same procedure as for the one-minute interval was practiced; i.e. average of the closest available pre and post timestamp measurement.

8.3.1 Wind driven gas exchange coefficient models

Five models, in which k_{600} is calculated from single parameter input U_{10} were used in this study:

- Power function as described by Cole and Caraco (1998):

  $$k_{600} = 2.07 + 0.215{U_{10}}^{1.7} \quad (5)$$

  where k_{600} is gas exchange coefficient (cm h^{-1}) and U_{10} is wind speed at 10 m height (m s^{-1}).
- Bilinear function as described by Crusius and Wanninkhof (2003). Two separate functions: one for wind speeds below 3.7 m/s (6) and one for all other wind speeds (7). Originally suggested by Liss and Merlivat (1986):

  $$k_{600} = 0.72U_{10} \quad (6)$$

  $$k_{600} = 4.33U_{10} - 13.3 \quad (7)$$

  where k_{600} is gas exchange coefficient (cm h^{-1}) and U_{10} is wind speed at 10 m height (m s^{-1}).

- Power function as described by Crusius and Wanninkhof (2003)

  $$k_{600} = 0.168 + 0.228{U_{10}}^{2.2} \quad (8)$$

  where k_{600} is gas exchange coefficient (cm h^{-1}) and U_{10} is wind speed at 10 m height (m s^{-1}).

- Constant and linear function as described by Crusius and Wanninkhof (2003). Two separate functions: one for wind speed below 3.7 m s^{-1} (9) and one for all other wind speed (10). Again, U_{10} is wind speed at 10 m height (m s^{-1}) and k_{600} is gas exchange coefficient (cm h^{-1}).

  $$k_{600} = 1.0 \quad (9)$$

  $$k_{600} = 5.14U_{10} - 17.9 \quad (10)$$

- Power function as described by Wanninkhof (1992). U_{10} is wind speed at 10 m height (m s^{-1}) and k_{600} is gas exchange coefficient (cm h^{-1}).

$$k_{600} = 0.45{U_{10}}^{1.64} \tag{11}$$

8.4 Wind speed at 10 meters

The wind speed measurements from Inre Harrsjön originate from two sonic anemometers mounted at 115 and 205 cm above lake surface respectively. Conversion to wind speed at 10 meters (U_{10}) was performed using wind speed transformation model (12) from Lundin et al. (2013):

$$U_{10} = U_z\left\{1 + \left[(C_{d10})^{1/2}/\kappa\right]\ln\left(\frac{10}{z}\right)\right\} \tag{12}$$

where U_{10} is wind speed (m s^{-1}) at 10 meters, U_z is wind speed (m s^{-1}) at sonic anemometer height z (m), C_{d10} is drag coefficient at 10 m (1.3×10^{-3}; Large and Pond, 1980), κ is the von Karman constant (0.41; Vachon et al., 2010) and z is sonic anemometer height (m) over lake surface. In calculation of wind speed at 10 meters, lake surface level was considered constant thus the previously mentioned heights were used for all conversions of measured wind speed to U_{10}. Time-interval U_{10} was calculated by averaging the sum of available measurements converted to U_{10}, i.e. every measurement within time-interval was converted to U_{10} before being summed up and averaged.

8.5 Finding best fit

Result from the combinations of models and temporal resolution was compared to the average of measurements for days where measurements were available. The absolute difference between modeled and measured results were summed and averaged per combination of model and temporal resolution. The combination of model and temporal resolution producing the least average absolute difference were considered the best-fit combination.

8.6 Averaging measured fluxes

Daily averages were calculated excluding daily min and max values. Negative values, as found on July 4th 2011 and on August 24th 2011, were considered anomalies and were excluded from averages. Seasonal fluxes were calculated by multiplying the number of days (120) of the season with the average value of daily measurements for the season.

8.7 Lake surface concentration – Inverse calibration

Surface concentration given as a broad range introduced the problem (or opportunity) of selecting the value to use in model calculations. Two methods were evaluated, *static* and *variable* surface concentration. Using the static concentration approach all fluxes were calculated assuming surface concentration of 1.15 µmol L^{-1}, the average of min and max from the given range. In the variable concentration approach surface concentrations were checked for correlation to wind speed (per k_{600} model) in an attempt to compensate for the possibility of the lake being unable to keep up with modeled k-values (see section 6.4), as well as pinpoint the surface concentration within the large range. To illustrate the correlation, piston velocities were calculated (daily resolution) for days where actual measurements were available. Instead of calculating the final flux from the piston velocity and concentrations, the piston velocity along with the measured concentration were used to find the surface concentration that (if present) would have resulted in the model producing the same flux as manually measured - an *ideal*, or *required*, surface concentration. Resulting concentrations along with daily average U_{10} were plotted with wind on x-axis (cause) and required concentration on y-axis (effect). Linear trend lines were created using Microsoft Excel and the equations of those trend lines were used throughout the modeling to calculate the *variable concentration* for any given day. For each model two variable concentration equations were created; one based on all combinations of wind speed and required concentration, and one where only the required concentrations within given surface concentration range were considered. The resulting variable concentration equations allow for calculating concentration outside given range. When used in the modeling, any value calculated lower than range min was set to range min, and any value greater than range max was set to range max.

9 Results

9.1 Wind speed and direction

Wind roses, Fig. 3, 4 and 5, compiled from study site high frequency wind data, years 2010 through 2012, provide an overview of dominating wind directions and velocities. For the three years, every single measurement available is represented; 21287550 measurements for 2010, 103339222 for 2011 and 45524876 for 2012. Size of wind speed bins was derived from classification used by the Swedish Meteorological and Hydrological Institute (SMHI, 2014). Difference in records used for the different year is related to up/down –time of measuring equipment. Values are as measured, i.e. not converted to U_{10}. It should be noted that although the results look similar across the years the result is based on the *good* data, i.e. the periods where sonic anemometers produced valid data.

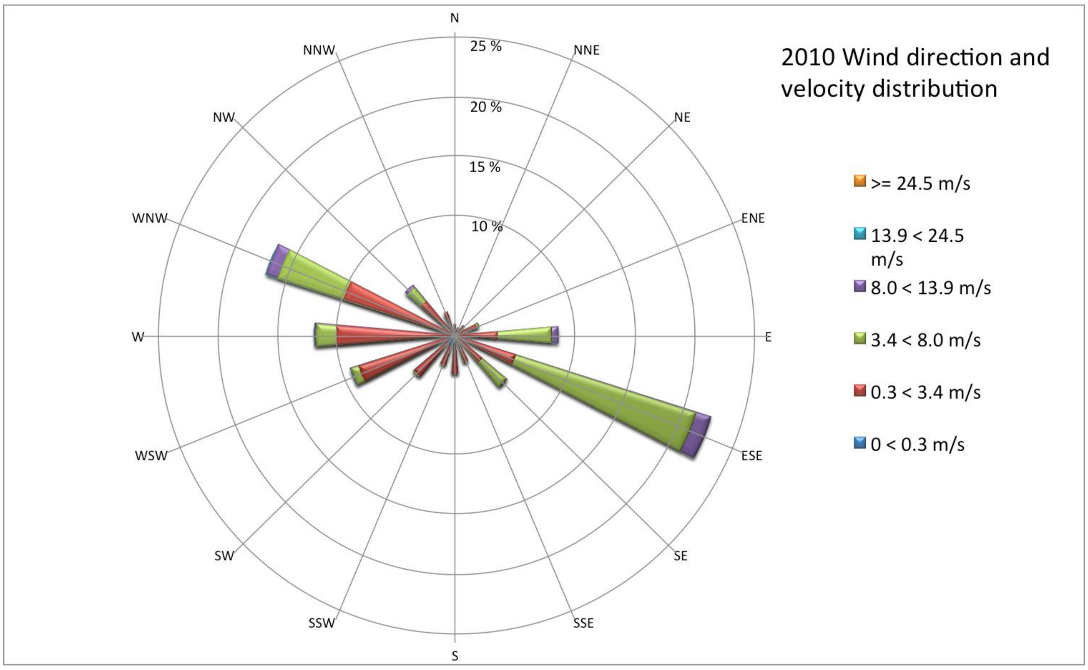

Figure 3. Inre Harrsjön wind direction and velocity distribution. Wind rose compiled from 21287550 individual records available for year 2010.

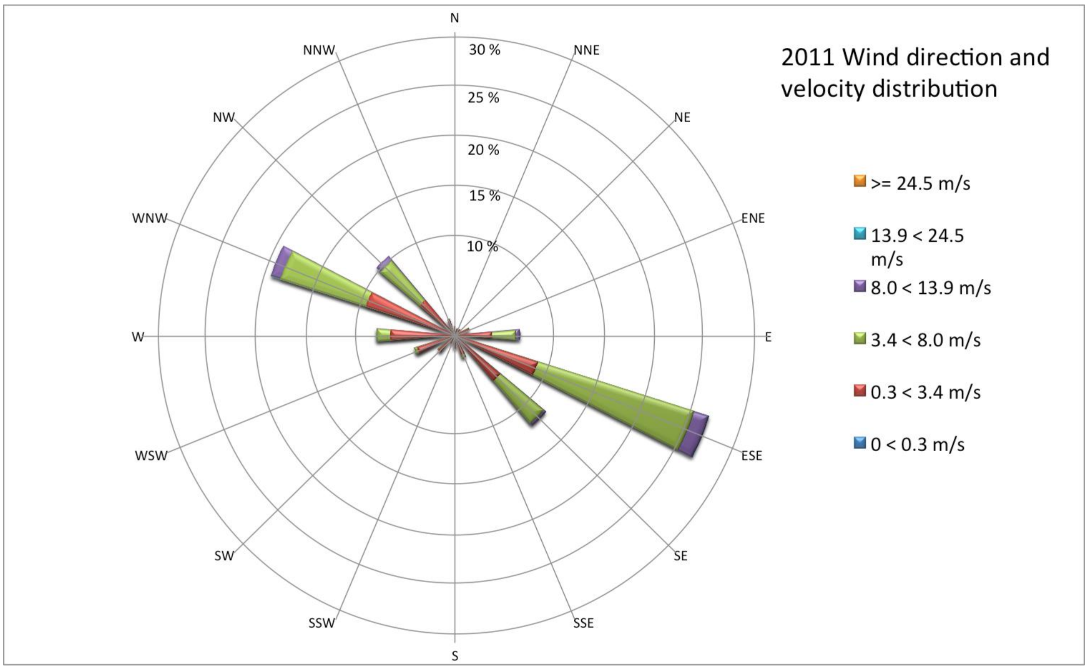

Figure 4. Inre Harrsjön wind direction and velocity distribution. Wind rose compiled from the 103339222 individual records available for year 2011.

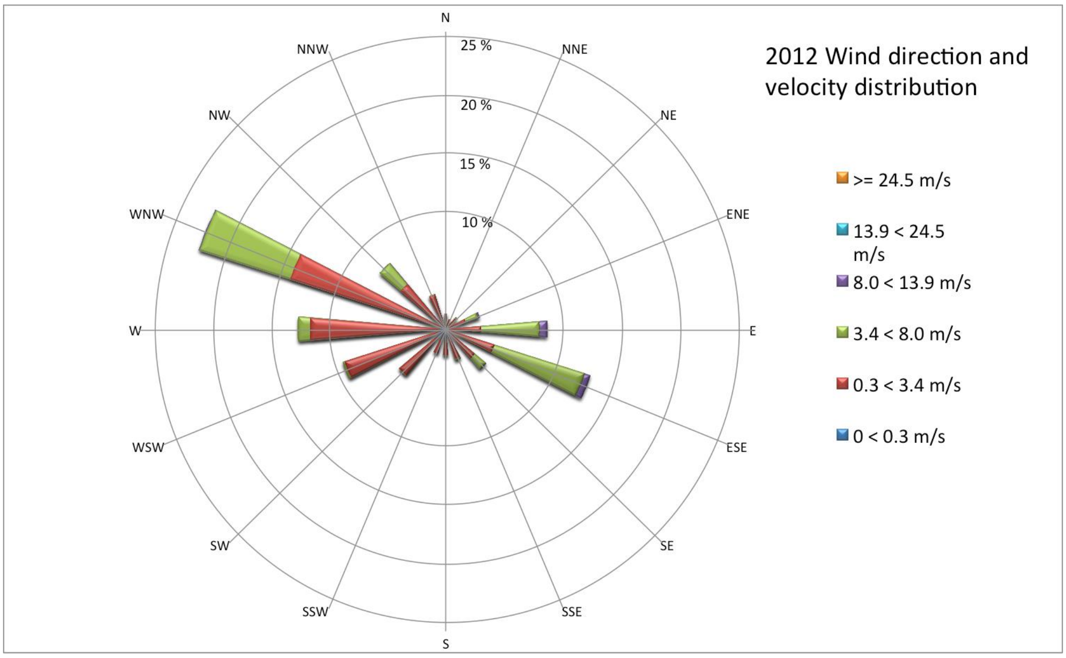

Figure 5. Inre Harrsjön wind direction and velocity distribution. Wind rose compiled from the 45524876 individual records available for year 2012.

9.2 Wind speed at 10 meters

Fig. 6 and Fig. 7 show the U_{10} values calculated for the two seven-day periods selected for fine resolution modeling (section 8.1.1). Following the logic presented in section 8.4, wind speeds indicated for any period is the result of averaging all (U_{10}-converted) values available during the period. For time intervals where two sonic anemometers were producing good data the one-minute interval is based on 2400 individual measurements, ranging up to 3456000 for the full-day interval.

For both seven-day intervals, wind speed in the finest resolution window (1 minute) range from ~ 0 m s^{-1} to just above 9 m s^{-1}. At full-day resolution wind speed minimum is raised and maximum is lowered, ranging from 1.5 m s^{1} to ~5.5 m s^{-1} for both periods. Generally, (per day) wind speed is low in early hours, builds up to a peak around noon and finally drops in the last hours of the day. As expected, variability decreases with increasing length of time period.

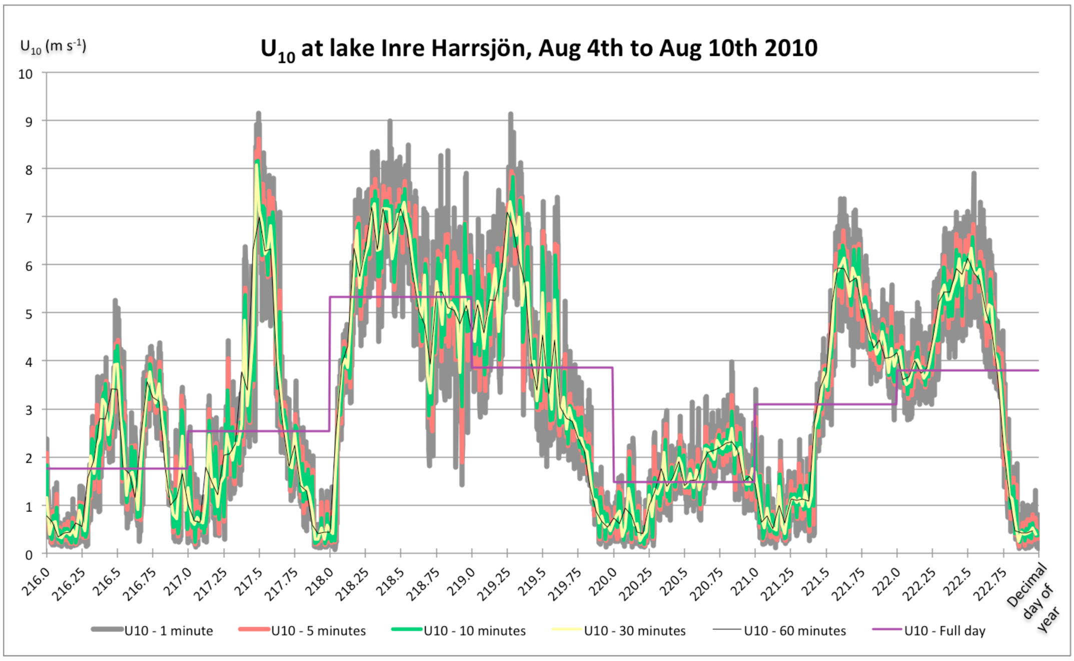

Figure 6. Inre Harrsjön. High frequency (20 Hz) wind measurements converted to U_{10} and averaged over several temporal resolutions. Data start at August 4th and end at August 10th, 2010.

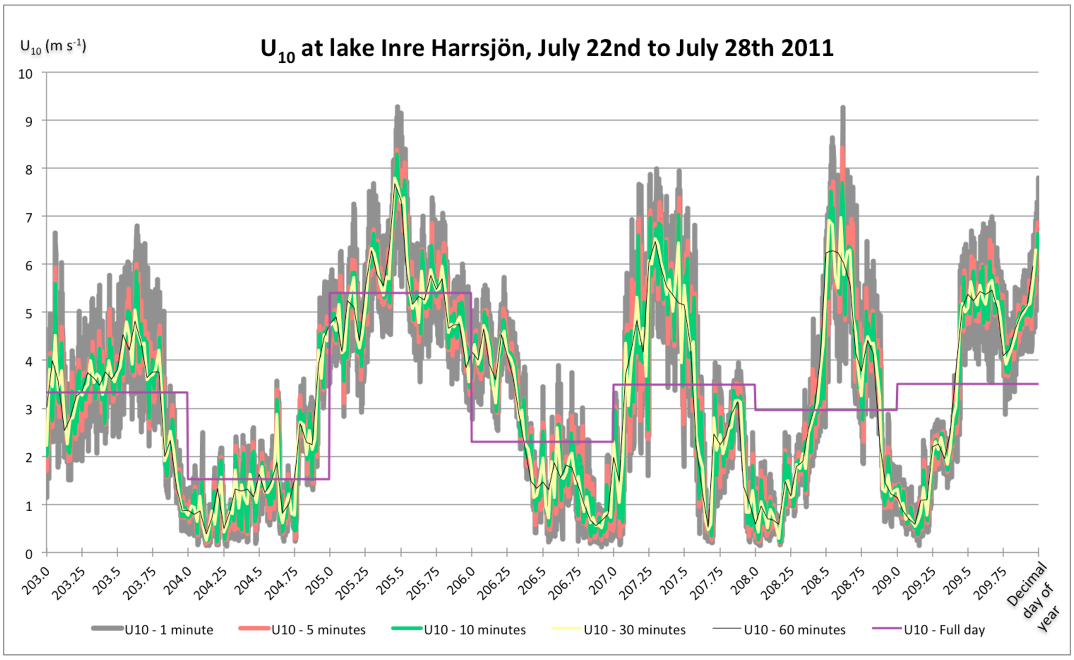

Figure 7..Inre Harrsjön. High frequency (20 Hz) wind measurements converted to U_{10} and averaged over several temporal resolutions. Data start at July 22nd and end at July 28th, 2011.

9.3 k_{600} – Piston Velocity

U_{10} values calculated for the different temporal resolutions served input for each of the k_{600} models evaluated. Min, max and average k_{600} figures for the two seven-day periods are listed in Table 2 and Table 3. Although the data is identical in the two tables the presentation differs. Table 2 allows for comparison between k_{600} results of the different models using same temporal resolution of input wind data. In Table 3 the results are presented with the intent of following changes in result produced from a single model across the studied temporal resolutions of input wind data.

Model specific results for the two seven-day periods are presented in appendix A, sections 14.2 and 14.3, with the results grouped per model. Each chart, Fig. A-1 through A-10, presents the result of a single model at all time spans evaluated.

As with the U_{10}, k_{600} variation decreases with increasing size of the averaging window. For all models, at both time periods, usage of one-minute wind data produced highest period average k_{600}. Full-day wind data produced the lowest period average k_{600}.

Table 2. Min, max and average k_{600} values modeled for two seven-day intervals using varying resolution on input wind data.

Min, max and average k_{600} (cm h^{-1}) during two seven-day intervals. Results calculated using input wind data at several temporal resolutions.																		
	U_{10} averaging window (measured @ 20 Hz)																	
	1 minute			**5 minutes**			**10 minutes**			**30 minutes**			**60 minutes**			**Full day**		
k_{600} model	min	max	avg	min	max	avg	min	max	avg	min	max	avg	min	max	avg	min	max	avg
Time period: August 4th to August10th, 2010																		
C&C-PW1998	2.073	11.332	3.987	2.077	10441	3.975	2.082	9.698	3.969	2.09	9.574	3.958	2.104	8.225	3.948	2.487	5.772	3.701
C&W-BL2003	0.055	26.311	4.766	0.1	24.023	4.726	0.133	22.038	4.709	0.179	21.697	4.675	0.243	17.848	4.645	1.063	9.798	3.252
C&W-PW2003	0.169	29.875	4.744	0.171	26.23	4.685	0.174	23.278	4.661	0.179	22.79	4.616	0.189	17.675	4.571	0.706	9.236	3.549
C&W-CL2003	1	29.121	4.597	1	26.404	4.541	1	24.049	4.517	1	23.644	4.469	1	19.075	4.426	1	9.518	2.443
W-PW1992	0.007	16.974	3.651	0.018	15.396	3.63	0.028	14.076	3.62	0.046	13.854	3.601	0.076	11.444	3.583	0.853	7.008	3.156
Time period: July 22nd to July 28th, 2011																		
C&C-PW1998	2.075	11.563	3.989	2.082	10.128	3.974	2.085	9.922	3.968	2.091	9.117	3.957	2.112	8.954	3.948	2.509	5.847	3.751
C&W-BL2003	0.083	26.891	4.599	0.132	23.196	4.538	0.149	22.644	4.513	0.181	20.429	4.474	0.275	19.967	4.432	1.096	10.07	3.202
C&W-PW2003	0.17	30.84	4.615	0.173	24.976	4.547	0.175	24.158	4.521	0.179	21.026	4.476	0.195	20.403	4.439	0.742	9.473	3.631
C&W-CL2003	1	29.809	4.263	1	25.423	4.175	1	24.767	4.141	1	22.139	4.085	1	21.59	4.027	1	9.842	2.263
W-PW1992	0.013	17.384	3.666	0.028	14.841	3.641	0.034	14.474	3.631	0.047	13.041	3.612	0.093	12.749	3.596	0.896	7.145	3.254

Table 3. Min, max and average k_{600} values modeled for two seven-day intervals using varying resolution on input wind data.

Min, max and average k_{600} (cm h^{-1}) during two seven-day intervals. Results calculated using input wind data at several temporal resolutions.															
U_{10} averaging window (measured @ 20 Hz)	**k_{600} (cm h^{-1}) per model**														
	C&C-PW1998			**C&W-BL2003**			**C&W-PW2003**			**C&W-CL2003**			**W-PW1992**		
	min	max	avg	min	max	avg	min	max	avg	min	max	avg	min	max	avg
Time period: August 4th to August 10th, 2010															
1 minute	2.073	11.332	3.987	0.055	26.311	4.766	0.169	29.875	4.744	1	29.121	4.597	0.007	16.974	3.651
5 minutes	2.077	10.441	3.975	0.1	24.023	4.726	0.171	26.23	4.685	1	26.404	4.541	0.018	15.396	3.63
10 minutes	2.082	9.698	3.969	0.133	22.038	4.709	0.174	23.278	4.661	1	24.049	4.517	0.028	14.076	3.62
30 minutes	2.09	9.574	3.958	0.179	21.697	4.675	0.179	22.79	4.616	1	23.644	4.469	0.046	13.854	3.601
60 minutes	2.104	8.225	3.948	0.243	17.848	4.645	0.189	17.675	4.571	1	19.075	4.426	0.076	11.444	3.583
Full day	2.487	5.772	3.701	1.063	9.798	3.252	0.706	9.236	3.549	1	9.518	2.443	0.853	7.008	3.156
Time period: July 22nd to July 28th, 2011															
1 minute	2.075	11.563	3.989	0.083	26.891	4.599	0.17	30.84	4.615	1	29.809	4.263	0.013	17.384	3.666
5 minutes	2.082	10.128	3.974	0.132	23.196	4.538	0.173	24.976	4.547	1	25.423	4.175	0.028	14.841	3.641
10 minutes	2.085	9.922	3.968	0.149	22.644	4.513	0.175	24.158	4.521	1	24.767	4.141	0.034	14.474	3.631
30 minutes	2.091	9.117	3.957	0.181	20.429	4.474	0.179	21.026	4.476	1	22.139	4.085	0.047	13.041	3.612
60 minutes	2.112	8.954	3.948	0.275	19.967	4.432	0.195	20.403	4.439	1	21.59	4.027	0.093	12.749	3.596
Full day	2.509	5.847	3.751	1.096	10.07	3.202	0.742	9.473	3.631	1	9.842	2.263	0.896	7.145	3.254

9.4 Variable surface concentration

The variable surface concentration evaluation was based around a total of 40 days on which both flux measurements and wind data were available. For each of the 40 days, the calculated k_{600} figures, per model, were used in search of the surface concentration that would have resulted in the modeled flux being equal to the actual measured flux of the day. Resulting *required* (or model-ideal) surface concentrations, along with daily average U_{10} are presented in Fig. 8 and Fig. 9. The figures also include model specific linear trend lines, which equations (Eq. 13 through 22) later were used in calculation of fluxes. Two sets of result were generated: one only containing required concentrations within original given range, and another where *all* required concentrations are present. The equations describing the possible relation between wind speed and ideal surface concentration differ slightly between the two approaches and final flux modeling was performed using both. The ten equations describing variable surface concentrations share variable naming convention: *c* is concentration in µmol L^{-1}, and U_{10} is wind speed at ten meters height in m s^{-1}. As already mentioned in section 8.7, the equations allow for resulting ideal concentrations being outside the given range, and in such cases, once used for producing model result, any concentration lower than range min was set to range min, and any concentration greater than range max was set to range max.

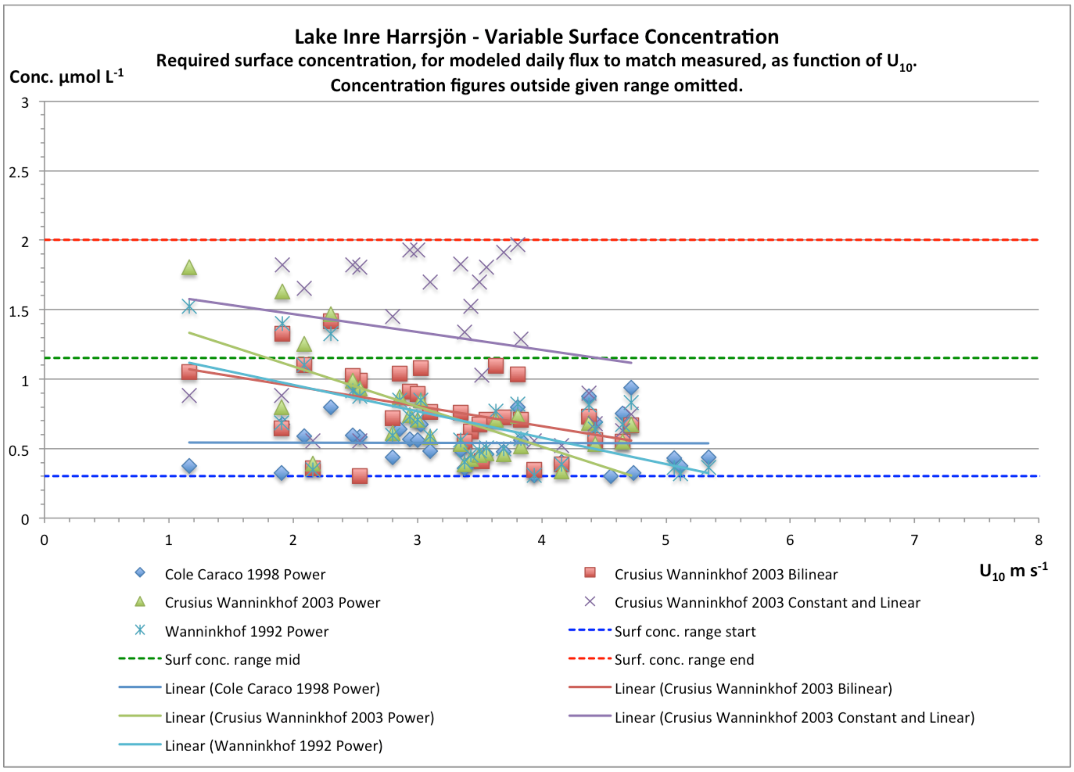

Figure 8. Lake surface concentration required for modeled fluxes to match actual measured fluxes as function of daily wind speed for five k_{600}-models. Original lake surface concentration range min and max values represented by dotted blue and red lines respectively. Chart only includes ideal lake surface concentration figures within the given range.

Variable concentration equations for *range-only* calculated concentrations (Fig. 8):

- Cole and Caraco, power function (1998)

$$c = -0.0015U_{10} + 0.5459 \quad (13)$$

- Crusius and Wanninkhof, bilinear function (2003)

$$c = -0.1443U_{10} + 1.2385 \quad (14)$$

- Crusius and Wanninkhof, power function (2003)

$$c = -0.289U_{10} + 1.6697 \quad (15)$$

- Crusius and Wanninkhof, constant and linear combination (2003)

$$c = -0.1292U_{10} + 1.7266 \quad (16)$$

- Wanninkhof, power function (1992)

$$c = -0.1901U_{10} + 1.3389 \quad (17)$$

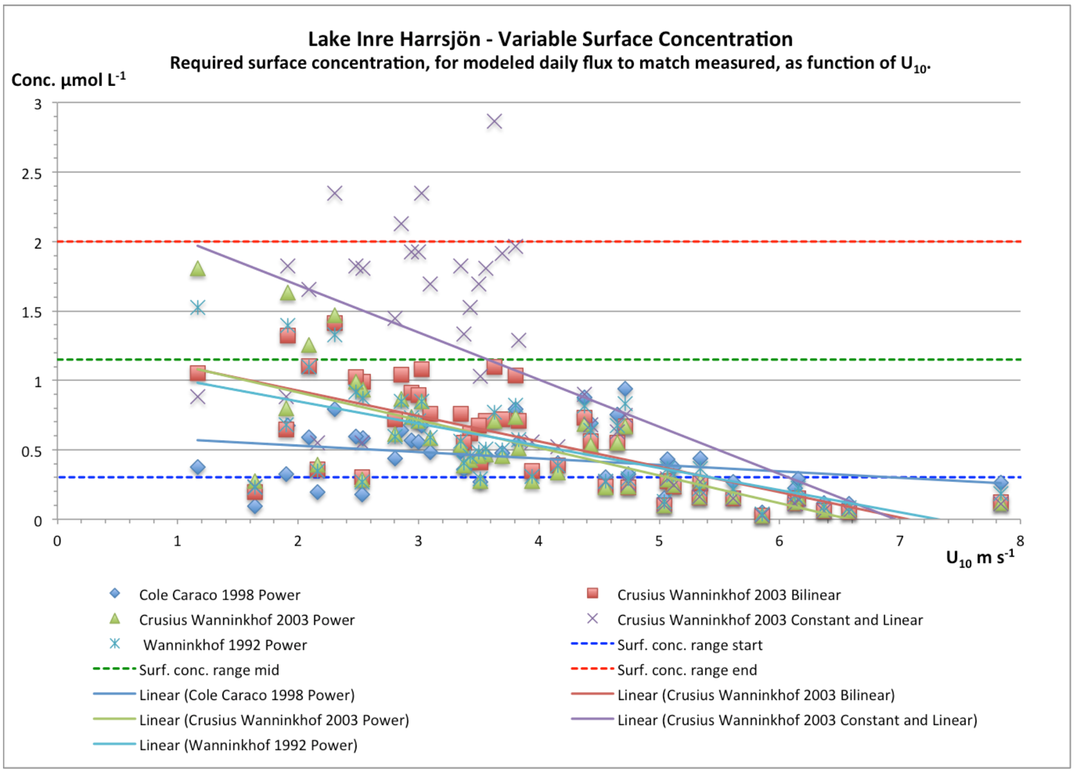

Figure 9. Lake surface concentration required for modeled fluxes to match actual measured fluxes, on 40 days, as function of daily wind speed for five k_{600}-models. Original lake surface concentration range min and max values represented by dotted blue and red lines respectively.

Variable concentration equations for *all* calculated concentrations (Fig. 9):

- Cole and Caraco, power function (1998)

$$c = -0.0464U_{10} + 0.6236 \quad (18)$$

- Crusius and Wanninkhof, bilinear function (2003)

$$c = -0.183U_{10} + 1.2929 \quad (19)$$

- Crusius and Wanninkhof, power function (2003)

$$c = -0.1996U_{10} + 1.3131 \quad (20)$$

- Crusius and Wanninkhof, constant and linear combination (2003)

$$c = -0.3399U_{10} + 2.3653 \quad (21)$$

- Wanninkhof, power function (1992)

$$c = -0.16U_{10} + 1.1697 \quad (22)$$

9.5 Comparing Modeled and Measured Fluxes

Modeled and measured fluxes for the days (within the two seven-day spans, section 8.1.1) where both high-frequency wind data and actual flux measurements were available are listed in Table 4. For comparison, Table 4 also lists the average absolute difference between modeled and measured diffusive flux per model and temporal resolution. Results were calculated using both static and variable concentration. Results ranging from 1 to 60 minutes were calculated using the static concentration approach. Since the variable concentration approach was based around daily flux measurements, no results were calculated for temporal resolution finer than full day. Two variable concentration equations were used per k_{600} model (section 9.4).

Static concentration approach

Using static concentration approach, the power function described by Wanninkhof (1992) (Eq. 11) fed by daily wind data results in diffusive fluxes closest to average of those measured. Model results generally exceed the average of measured fluxes, however the two models based around linear relationship between wind speed and gas flux, Crusius and Wanninkhof Bilinear (Eq. 6 and 7) and Constant and Linear (Eq. 9 and 10) are much more restrictive in their estimates when ran on daily resolution. On five of the six evaluated dates these two models produce the lowest flux estimates. On August 6th 2010 all modeled result end up several factors larger than the average of measured fluxes. Fig. 6 (section 9.2) shows this day had the highest daily wind speed of the dates evaluated for 2010. Section 6.4 briefly touches on the topic of possible CH_4 release, from lake to atmosphere, being connected to the CH_4 producing processes in the sediment layer; sustained high k-values could (temporarily) deplete the lake storage effectively capping the possible flux. Motivated by this “flux capacity”, the average absolute difference between modeled and measured fluxes was recalculated excluding August 6th 2010. Results from calculation excluding August 6th 2010 are also listed in Table 6. With the exclusion of the high wind date all models predicts values closer to measured flux, and the two linear-based models stand out as top performers being 2.32 and 2.64 mg m^{-2} d^{-1} off from average measured fluxes.

Variable concentration approach

Applying the variable concentration equations to the flux models resulted in a significant drop in estimated fluxes produced by all evaluated models. Similar to the static concentration approach, although not as dramatic, excluding the high-wind date (August 6th 2010) resulted in a drop in average absolute difference from measured fluxes.

Table 4. Measured and modeled diffusive CH_4 flux for days where both flux measurements and high-frequency wind data were available. Where not noted otherwise, calculated fluxes where calculated using static surface concentration approach. *Variable surface concentration based on *range-only* calculated required surface concentrations. **Variable surface concentration based on *all* calculated required surface concentrations

Measured / model name / resolution	Diffusive lake to atmosphere CH_4 flux (mg m^{-2} d^{-1})							
	05/08/10	06/08/10	09/08/10	10/08/10	25/07/11	01/08/11	Avg. abs diff from measured: Including 06/08/10	Avg. abs diff from measured: Excluding 06/08/10
Average (excluding min and max) from chamber measurements								
Daily	5.92	5.06	5.69	11.44	7.5	4.62	-	-
Cole Caraco 1998 Power								
1 Minute	13.56	23.46	15.51	17.8	11.83	15.93	9.64	7.89
5 Minutes	13.51	23.38	15.48	17.76	11.8	15.89	9.6	7.85
10 Minutes	13.49	23.34	15.47	17.75	11.78	15.88	9.58	7.84
30 Minutes	13.43	23.3	15.45	17.74	11.76	15.83	9.55	7.81
60 Minutes	13.36	23.26	15.43	17.73	11.71	15.83	9.51	7.78
Full day	11.73	22.55	13.65	16.57	10.86	15.01	8.36	6.53
Full day*	5.51	10.51	6.4	7.76	5.1	7.04	2.51	1.92
Full day**	5.14	7.33	5.67	6.41	4.86	6.07	2.03	1.98
Crusius Wanninkhof 2003 Bilinear								
1 Minute	14.48	41.42	17.93	23.28	8.45	15.15	13.41	8.82
5 Minutes	14.32	41.18	17.83	23.05	8.33	14.71	13.2	8.61
10 Minutes	14.24	41.08	17.8	22.96	8.28	14.47	13.1	8.52
30 Minutes	14.05	40.9	17.8	22.91	8.28	14.13	12.97	8.4
60 Minutes	13.71	40.8	17.71	22.81	8.08	14.01	12.81	8.23
Full day	6.88	38.28	8.61	12.72	6.09	9.68	7.47	2.32
Full day*	5.21	15.53	5.91	7.61	4.79	6.31	3.27	1.83
Full day**	4.95	10.46	5.42	6.57	4.61	5.66	2.57	2.01
Crusius Wanninkhof 2003 Power								
1 Minute	14.31	40.96	17.85	23.6	8.88	16.96	13.72	9.29
5 Minutes	14.08	40.49	17.69	23.36	8.75	16.76	13.48	9.09
10 Minutes	13.99	40.3	17.63	23.29	8.69	16.7	13.39	9.03
30 Minutes	13.72	40.04	17.56	23.23	8.61	16.57	13.25	8.9
60 Minutes	13.35	39.77	17.48	23.17	8.48	16.49	13.08	8.76
Full day	7.28	36.08	11.24	17.9	5.87	13.88	9.21	4.85
Full day*	5.93	9.33	7.55	8.83	5.12	8.35	2.48	2.12
Full day**	5.1	9.33	6.77	8.58	4.35	7.69	2.54	2.2
Crusius Wanninkhof 2003 Constant and Linear								
1 Minute	14.46	41.7	16.9	21.75	6.96	11.79	12.4	7.56
5 Minutes	14.23	41.35	16.76	21.43	6.79	11.16	12.15	7.32
10 Minutes	14.12	41.22	16.72	21.31	6.72	10.83	12.04	7.22
30 Minutes	13.84	40.94	16.7	21.23	6.72	10.34	11.85	7.05
60 Minutes	13.36	40.8	16.58	21.09	6.43	10.16	11.72	6.92
Full day	3.77	37.18	3.86	6.68	3.67	3.98	7.56	2.64
Full day*	4.58	33.53	4.45	7.18	4.56	4.46	6.4	1.99
Full day**	4.93	17.79	4.4	6.22	5.05	4.21	3.85	2.07
Wanninkhof 1992 Power								
1 Minute	10.87	28.98	14.14	18.35	8.04	14.6	9.13	6.17
5 Minutes	10.78	28.84	14.08	18.26	7.98	14.53	9.04	6.09
10 Minutes	10.74	28.78	14.06	18.24	7.94	14.5	9.01	6.06
30 Minutes	10.63	28.7	14.03	18.22	7.9	14.44	8.95	6.01
60 Minutes	10.5	28.62	13.99	18.2	7.82	14.42	8.89	5.95
Full day	7.8	27.38	11.09	16.08	6.5	13.19	7.3	4.3
Full day*	5.8	7.67	7.22	8.57	5.08	7.97	2.15	2.06
Full day**	5.17	7.47	6.49	7.81	4.52	7.19	2.19	2.15

9.6 Four years of diffusive fluxes

As a final step in evaluating diffusive CH_4 release from the lake, fluxes were modeled for the (approximately) ice-free seasons (June 1st – September 28th) of years 2009 through 2012. Fluxes were calculated on daily resolution as well as on full season. Full season result is based on seasonal average input values, i.e. every input parameter averaged over entire season before fed into respective model. Results were produced using both static concentration (Table 5) and the two variable concentration approaches (Table 6 and 7). Tables listing these fluxes also present the daily measurements up-scaled to full season (see section 8.4) allowing comparison between modeled and measured values. For year 2009 there was no measured flux data available.

Seasonal fluxes calculated using static concentrations (Table 5) generally end up several factors larger than the measured fluxes, and do so regardless of temporal resolution. The only exception is the constant and linear model (Crusius and Wanninkhof, 2003) (Eq. 9 and 10) which shows significant drop in estimated flux when going from daily resolution to full season.

In results produced from the application of variable surface concentration (Table 6 and 7), the seasonal fluxes come closer to the up-scaled daily measured values. Per model, the result for the four years, are also closer: the resulting range for results modeled for the four years is a lot tighter. Again, the constant and linear model (Crusius and Wanninkhof, 2003) (Eq. 9 and 10) seems least consistent in its resulting fluxes.

In Table 8 the modeled fluxes are presented (model/resolution/concentration) as percentage of the up-scaled measurements for the three seasons where chamber measurement data were available. Model fluxes drop significantly with the introduction of the variable concentration approach (both).

Table 5. Four years of modeled and measured diffusive CH_4 fluxes from Inre Harrsjön calculated using static surface concentration approach.

Flux source	Resolution	Diffusive CH_4 flux (mg m^{-2}) per season (120 days)			
		Season 2009	Season 2010	Season 2011	Season 2012
Measured avg.	Daily	-	786	686	644
Cole Caraco 1998 Power	Daily	1896	2147	2266	1810
Crusius Wanninkhof 2003 Bilinear	Daily	2214	3332	3334	2196
Crusius Wanninkhof 2003 Power	Daily	2381	3416	3369	2305
Crusius Wanninkhof 2003 Const and Linear	Daily	1870	3223	3131	1919
Wanninkhof 1992 Power	Daily	1928	2481	2553	1842
Cole Caraco 1998 Power	Season	1871	2095	2140	1608
Crusius Wanninkhof 2003 Bilinear	Season	1610	2876	2743	1056
Crusius Wanninkhof 2003 Power	Season	2094	2887	2836	1669
Crusius Wanninkhof 2003 Const and Linear	Season	984	2531	2324	398
Wanninkhof 1992 Power	Season	1856	2348	2345	1522

Table 6. Four years of modeled and measured diffusive CH_4 fluxes from Inre Harrsjön. Fluxes calculated using variable concentration approach based on *range-only* ideal surface concentrations.

Flux source	Input Resolution	Diffusive CH_4 flux (mg m^{-2}) per season (120 days)			
		Season 2009	Season 2010	Season 2011	Season 2012
Measured avg.	Daily	-	786	686	644
Cole Caraco 1998 Power	Daily	886	1000	1057	846
Crusius Wanninkhof 2003 Bilinear	Daily	1022	1234	1282	988
Crusius Wanninkhof 2003 Power	Daily	928	1060	1103	860
Crusius Wanninkhof 2003 Const and Linear	Daily	1651	2514	2621	1686
Wanninkhof 1992 Power	Daily	852	859	920	778
Cole Caraco 1998 Power	Season	877	976	1000	753
Crusius Wanninkhof 2003 Bilinear	Season	940	1410	1398	646
Crusius Wanninkhof 2003 Power	Season	975	804	899	872
Crusius Wanninkhof 2003 Const and Linear	Season	1044	2475	2313	432
Wanninkhof 1992 Power	Season	956	920	979	841

Table 7. Four years of modeled and measured diffusive CH_4 fluxes from Inre Harrsjön calculated from variable surface concentration. Surface concentration calibrated on full (range ignored) model-to-measure correlation.

Flux source	Input Resolution	Diffusive CH_4 flux (mg m^{-2}) per season (120 days)			
		Season 2009	Season 2010	Season 2011	Season 2012
Measured avg.	Daily	-	786	686	644
Cole Caraco 1998 Power	Daily	695	712	765	660
Crusius Wanninkhof 2003 Bilinear	Daily	874	1057	1082	830
Crusius Wanninkhof 2003 Power	Daily	910	1055	1086	840
Crusius Wanninkhof 2003 Const and Linear	Daily	1049	1313	1297	1041
Wanninkhof 1992 Power	Daily	790	821	874	725
Cole Caraco 1998 Power	Season	715	738	767	630
Crusius Wanninkhof 2003 Bilinear	Season	804	1094	1111	565
Crusius Wanninkhof 2003 Power	Season	963	955	1013	833
Crusius Wanninkhof 2003 Const and Linear	Season	884	1716	1681	383
Wanninkhof 1992 Power	Season	873	861	910	764

Table 8. Modeled seasonal diffusive CH_4 flux as percent of measured flux.
* Modeled value established using variable lake surface concentration based on range-only ideal concentrations. ** Modeled value established using variable lake surface concentration based on full set of ideal concentrations.

Model	Conc. calibration approach	Input Resolution	Modeled seasonal CH_4 diffusive flux as percent of measured		
			Season 2010	Season 2011	Season 2012
Cole Caraco 1998 Power	Static	Daily	273	330	281
		Season	267	312	250
	Variable*	Daily	127	154	131
		Season	124	146	117
	Variable**	Daily	91	112	102
		Season	94	112	98
Crusius Wanninkhof 2003 Bilinear	Static	Daily	424	486	341
		Season	366	400	164
	Variable*	Daily	157	187	153
		Season	179	204	100
	Variable**	Daily	134	158	129
		Season	139	162	88
Crusius Wanninkhof 2003 Power	Static	Daily	435	491	358
		Season	367	413	259
	Variable*	Daily	135	161	134
		Season	102	131	135
	Variable**	Daily	134	158	130
		Season	122	148	129
Crusius Wanninkhof 2003 Const and Linear	Static	Daily	410	456	298
		Season	322	339	62
	Variable*	Daily	320	382	262
		Season	315	337	67
	Variable**	Daily	167	189	162
		Season	218	245	59
Wanninkhof 1992 Power	Static	Daily	316	372	286
		Season	299	342	236
	Variable*	Daily	109	134	121
		Season	117	143	131
	Variable**	Daily	104	127	113
		Season	110	133	119

10 Discussion

Recapitulating the goal stated in the introduction, target of this exercise was to evaluate if any of the models considered, using the available measured data, would be suitable for use in extrapolation of diffusive CH_4 fluxes from the lake studied. Before any significance is attributed to the final results, the relevance of input variable selection and quality should be mentioned.

The diffusive gas flux (Eq. 1) is driven by piston velocity and the difference between lake surface and air-equilibrium gas concentrations. As seen in the temporal resolution analysis, the length of study interval influences model results. With wind data, being the main driver of piston velocity, used throughout the modeling originally sampled (at least) at every 30 minutes there is not much room for uncertainty of the k-values produced. The concentrations however, originally given as a range (lake surface) and a static value (air-equilibrium), introduce the possibility of great variance in final fluxes. With the air-equilibrium concentration being 3 nmol L^{-1}, compared to the range min 0.3 μmol L^{-1} of the lake surface concentration, its effects on final fluxes are limited. On the other hand, lake surface concentration greatly influences the final gas fluxes calculated, and as shown in 9.4, on almost every date where manual measurements were available, modeled fluxes could match these measured results by using a surface concentration within the given range.

Trusting the quality of the input data still leaves the problem of temporal resolutions, or rather lack of. Combining high frequency meteorological measurements with lake concentration data lacking temporal resolution in modeling which results are to be compared with daily manual measurements is easy to question. What conditions are responsible for the variance in surface concentration? When is surface concentration at its lowest and when is it at range max? With this problem acknowledged, focus can be shifted to the results produced.

Study-resolution

The high frequency wind analysis presented in section 9.2 shows that the wind, during the day, vary greatly. Even at 60-minute resolution U_{10} exhibit rapid changes. At finer resolutions, it seems unlikely that the lake would respond in a fashion similar to the almost on/off behavior of the measured wind. In the concept of piston velocity I imagine a spool-up time, or, the piston velocity being the result of ~continuous wind: a burst of high wind might not immediately translate (physically) to modeled piston velocity. This could well suggest daily resolution as least temporal unit for flux modeling. The daily resolution on manual measurements supports evaluation of models on daily resolution as well, but both finer and coarser sampling would have been useful.

Measured fluxes

On a total of 40 dates, over years 2010 through 2012, gas fluxes were measured at the lake (Table A-1). A closer look at the measured values reveals an obstacle with modeling of the lake behavior. On several of the dates, the minimum chamber measurement is by several factors separated from the maximum. Also, min and max measurements aren't necessarily bound to specific chambers, instead they shift between each measurement. Gas flux from the lake is not uniform; it varies both within dates, and across measuring chambers. Still, this evaluation required the lake to be treated as single uniform-acting unit. Excluding measured min and max from flux averages brought the daily fluxes closer, and the seasonal averages are not separated far. With only ~10% of days per season having actual measurements it can be argued that the selection of days isn't representative, which also would be reflected in the up-scaling from seasonal-average daily to full seasonal flux. It could also be argued that the gas flux from the lake not at all should, or even can, be treated as uniform. With the average fluxes for the three seasons (Table A-1) being so close (within ~10% of their average), perhaps this method only establishes a lake base-gas-flux, in which the (possible) importance of extreme high and low measurements isn't accounted for.

Variable concentrations approach

The equations in section 9.4, describing surface concentrations variations as function of wind, all express the need for lake surface concentrations to drop in order modeled values to match daily average measured gas flux. The two variations of variable concentration approach (using *all* values or *range-only* required concentrations) produce similar results with wind influence of required concentration being somewhat increased in the *all values* approach. Of the linear trend lines, and corresponding equations, in Fig. 5 and Fig. 6, three models (Crusius and Wanninkhof, power (2003)(Eq. 8); Crusius and Wanninkhof, bilinear (2003)(Eq. 6 and 7); Wanninkhof, power (1992)(Eq. 11)) display similar (assumed / presumed) correlation between required surface concentration and measured wind. The constant and linear k_{600}-model (Crusius and Wanninkhof, 2003)(Eq. 9 and 10) generates a variable required surface concentration much more dependent on wind conditions. Also, quickly eyeballing the scatterplots in Fig. 5 and Fig. 6 reveals this model as worst candidate for the variable concentration approach with charted points clouded around, instead of closer to, the trend line. The fifth and final model, the power function by Cole and Caraco (1998)(Eq. 5), requires almost no drop in surface concentration with increasing wind speed. In the *all values* approach the dependency on wind for this model is at least four times smaller than that of the other. Using range-only required surface concentrations, the effect of wind on surface concentration is almost entirely gone and the model produce (perfect) results using a ~ static (although lower than the static range mean) surface concentration.

A final look at the Fig. 5 and Fig. 6 illustrate problems already mentioned in 8.7; the variable concentration equations allows for calculation of required (ideal) concentrations outside range and for the equations there is a maximum wind which if exceeded would result in required concentrations ending up negative. In the modeling of seasonal fluxes the required surface concentrations were capped at min and max original concentration range. Any value less than min were set to min, any value greater than max were set to max. Another way around the problem would have been to define a *wind speed range* for each of the variable concentration equations, however this would still leave the task of handling wind outside the range.

Seasonal Fluxes

Already having seen the possible lack of fit from daily fluxes produced using the static surface concentration approach (Table 4), it isn't too surprising to see that the seasonal fluxes in Table 5 further suggest that this approach might not be suitable for modeling the lake behavior. Similar to the data in Table 4 modeled fluxes are 2-3 times greater than the up-scaled measured fluxes. This is descriptive for all models, regardless of modeling resolution (day/full season), with the single exception of the constant and linear model (Crusius and Wanninkhof, 2003)(Eq. 9 and 10), which shows a significant drop, from 1919 to 398 mg m^{-2}, for season 2012 when changing modeling resolution from daily to seasonal average. The drop in model result with increasing modeling resolution is present in the other model's results as well, but not as dramatic as for the constant and linear. Continuing with the two variable concentration approaches Table 6 holds the results calculated using *range only* (section 9.4) variable concentration equations. All models are significantly closer to measured fluxes, with the exception (again) of the constant and linear model (Crusius and Wanninkhof, 2003)(Eq. 9 and 10) which result is hard to interpret. Its result is the highest among the models, except for season 2012 where its value calculated for seasonal resolution is by far the smallest among the models. Finally, in Table 7, with results based on variable concentration equations derived from *all* (section 9.4) required concentrations, the modeled fluxes all take a step closer to the measured values with the constant and linear (Crusius and Wanninkhof, 2003)(Eq. 9 and 10) still being problematic. The aforementioned drop in flux when moving to coarser modeling resolution is now gone. The power function by Cole and Caraco (1998) (Eq. 5) produce lower fluxes when fed by daily resolution data for three out of the four seasons, and the power function by Wanninkhof (1992) (Eq. 11) do this for all four seasons. Although all the models produce result closer to the up-scaled measured flux, the power function by Cole and Caraco (1998)(Eq. 5) stand out as top performer. Whether daily modeling resolution is to be preferred over seasonal isn't easy to decide. If considering the average absolute difference between modeled and measured fluxes (as in the high frequency result), results built using seasonal input data end up closer to measured fluxes, however, the poor seasonal performance of the constant and linear model (Crusius and Wanninkhof, 2003)(Eq. 9 and 10) along with the fact that the chamber measurements (crucial for of the inverse calibration of concentration) was performed on daily basis suggests that daily modeling resolution is to be preferred.

11 Conclusion

Although not of scientific importance, the task of handling the huge amounts of measurements available for this thesis may be worth mentioning. The (somewhat tedious) creation of the database, loading of data, and implementation of software representing the piston velocity models really enabled this evaluation. Once completed, the software solution proved flexible and easily extendable with new features. The introduction of variable concentration was incorporated in a matter of hours. Any future similar studies are likely to benefit from the database already existing. Also, given the need, the dataset can well be completed with further measurements.

Based around meteorological data sampled at various rates, five piston velocity models were evaluated with the purpose of finding the model, along with temporal resolution, best matching the measured diffusive CH_4 release from the small subarctic lake Inre Harrsjön, Sweden. In crude simplification, this lake-to-atmosphere diffusive flux can be said to depend on piston velocity and lake surface (CH_4) concentration. With surface concentration, from the perspective of this modeling, being available only as a broad range, modeled fluxes is greatly depending on concentration selected at model run. Two approaches on how to treat lake surface concentration were evaluated.

In a first run fluxes were modeled using static surface concentration (range average) and high frequency wind data (20 Hz). Results were modeled for 1, 5, 10, 30, 60 and 1440 minutes (full day) and compared to measured results of corresponding dates. Although modeled values dropped with increasing temporal calculation window the result generally ended up several factors larger than average measured daily fluxes. With the 20 Hz data lacking in availability, as well as the processing power associated with the (large) size of the dataset, the poor results provided motivation in proceeding analysis using wind data sampled at 30 minutes resolution. From the 30-minute data, daily fluxes were modeled and summarized for the four full seasons (120 days) of years 2009, 2010, 2011 and 2012. Up-scaling the available (per season) chamber measurements allowed for comparison between modeled and (up-scaled) actual fluxes. Again the modeled values were too optimistic. Seasonal fluxes were also modeled using seasonal average parameter values. Seasonal resolution of input parameters brought model result somewhat closer to the up-scaled chamber measurements, however the modeled fluxes were still of by 2~3 factors.

Attempting to improve model performance in following iterations, static lake surface concentration was abandoned for a variable concentration approach. This variable surface concentration approach was based around the inversion of the lake-atmosphere interface flux equation, i.e. instead of modeling the diffusive flux, the gas exchange equation was used to establish the surface concentration required in order for the modeled fluxes to reach the average of measured fluxes on a date. These required, or ideal, concentrations were calculated for all five models on the 40 dates through 2010 to 2012 where chamber measurements were available. Required (ideal) concentrations (per model) were plotted as function of daily U_{10}. Equations of linear trend lines describing the correlation between required (ideal) concentrations and daily wind speed were incorporated into the flux calculations thus replacing static concentration with wind-controlled variable concentration. Per model, two variable concentration equations were established; one based on required concentrations within original given surface concentration range and one where any required concentration figure were taken into account. With the exception of the constant and linear model (Crusius and Wanninkhof, 2003)(Eq. 9 and 10) run on seasonal input data, models evaluated responded well to the variable concentration approach and resulting seasonal figures are significantly closer to the up-scaled chamber measurements, both using daily and seasonal input data.

As stated in the introduction, the aim of this evaluation was to find which, if any, of the chosen models could be used to predict the diffusive gas flux from the lake. Using the static concentration approach, none of the models produced figures close to those measured. With the introduction of variable concentration, all evaluated models to arrive at figures close to the up-scaled measured. Knowing this, the initial goal of finding a top-performing model must be extended to also include the way to perform the modeling; input resolution must be chosen, lake surface concentration must be handled. With only two options evaluated, the selection of lake surface concentration is easy since the numbers produced using the variable approach far surpassed the static approach in mimicking the measured fluxes. As for input resolution, the selection isn't as obvious. Motivated by the fact that chamber measurements were performed on daily basis, the recommendation is to run the models on daily resolution. Doing so also avoids problematic drop in result that the constant and linear model (Crusius and Wanninkhof, 2003)(Eq. 9 and 10) produced for 2012 using seasonal input data. In conclusion, the model most suitable for describing the diffusive CH_4 gas flux from Inre Harrsjön is the power function (Eq. 5) by Cole and Caraco (1998) fed by daily input data using variable concentration equation based on correlation between daily U_{10} and (any) required (ideal) concentration (Eq. 18), effectively removing the need for any detailed (the range is enough) knowledge of lake surface concentration. Seasonal fluxes modeled using this method are within ~ 10% of up-scaled chamber measurements. Ironically, this piston velocity model is by far the least wind dependent (of those evaluated) in its variable concentration equations. As in any modeling of nature, simplifications are present. In this exercise, up-scaling a few actual measurements to full seasons may not represent the actual behavior of the lake. However, the results gained from combining variable concentrations with the power function by Cole and Caraco (1998) (Eq. 5), or the power function by Wanninkhof (1992) (Eq. 11), suggests that modeling of diffusive lake-to-atmosphere fluxes benefit greatly from the implementation of inverse calibration of surface concentration, as described here. The inverse calibration of surface concentration, essentially representing the surface renewal processes without including turbulence physics, may well be applicable outside the studied lake.

12 Acknowledgements

My warmest hugs goes to Brett Thornton and Patrick Crill at Stockholm University. Thank you for entrusting me with all your measurements, the task of sorting them out, and for keeping me going (in the right direction). Also, big thanks to Martin Wik at Stockholm University for scouting even more data, and for the ever valuable lunch discussions.

13 References

Aubinet M., et al. (eds.) (2012), Eddy Covariance: A Practical Guide to Measurement and Data Analysis, Springer Atmospheric Sciences, pages 71, 80, doi:10.1007/978-94-007-2351-1

Callaghan V. T., Bergholm F., Christensen R. T., Jonasson C., Kokfelt U., and Johansson M. (2010), A new climate era in the sub-arctic: Accelerating climate changes and multiple impacts, Geophysical research letters, Vol. 37, L14705, pages 1-6, doi:10.1029/2009GL042064

Christensen R. T., Johansson T., Åkerman H. J., Mastepanov M., Malmer N., Friborg T., Crill P., and Svensson H. B. (2004), Thawing sub-arctic permafrost: Effects on vegetation and methane emissions, Geopysical Research Letters, Vol. 31, L04501, pages 1-4, doi:10.1029/2003GL018680

Ciais P., Sabine C., Bala G., Bopp L., Brovkin V., Canadell J., Chhabra A., DeFries R., Galloway J., Heimann M., Jones C., Le Quéré C., Myneni R.B., Piao S., and Thornton P. (2013), 2013: Carbon and Other Biogeochemical Cycles. In: Climate Change 2013: The Physical Science Basis. Contribution of Working Group I to the Fifth Assessment Report of the Intergovernmental Panel on Climate Change [Stocker T.F., Qin D., Plattner G. K., Tignor M., Allen S.K., Boschung J., Nauels A., Xia Y., Bex V., and Midgley P.M. (eds.)]. Cambridge University Press, Cambridge, United Kingdom and New York, NY, USA.

Cole J. J., Bade D. L., Bastviken D., Pace M. L., and Van de Bogert M. (2010), Multiple approaches to estimating air-water gas exchange in small lakes, Limnology and Oceanography: Methods, Vol. 8, pages 285-293

Cole J. J., and Caraco N. F. (1998), Atmospheric exchange of carbon dioxide in a low-wind lake measured by the addition of SF_6, Limnol. Oceanogr. Vol. 43, pages 647-656

Crusius J., and Wanninkhof R. (2003), Gas transfer velocities measured at low wind speed over a lake, Limnol. Oceanogr., Vol 48, pages 1010-1017

Guérin F., Abril G., Serça D., Delon C., Richard S., Delmas R., Tremblay A., and Varfalvy L. (2007), Gas transfer velocities of CO2 and CH4 in a tropical reservoir and its river downstream, Journal of Marine Systems Vol. 66, Pages 161–172

Huttunen J. T., Väisänen T. S., Hellsten S. K., and Martikainen P. J. (2006), Methane fluxes at the sediment–water interface in some boreal lakes and reservoirs. Boreal Env. Res. 11, pages 27–34.

Karlsson J., Christensen T. R., Crill P., Förster J., Hammarlund D., Jackowicz‐Korczynski M., Kokfelt U., Roehm C., and Rosén P. (2010), Quantifying the relative importance of lake emissions in the carbon budget of a subarctic catchment, J. Geophys. Res., 115, G03006, doi:10.1029/2010JG001305.

Liss P.S., and Slater P.G. (1974), Flux of Gases across the Air-Sea Interface, Nature, Vol. 247, pages 181-184

Large W.G., and Pond S. (1980), Open ocean momentum flux measurements in moderate to strong winds, Journal of Physical Oceanography, Vol. 11, pages 324-336

Lundin E. J., Giesler R., Persson A., Thompson M. S., and Karlsson J. (2013), Integrating carbon emissions from lakes and streams in a subarctic catchment, Journal of Geophysical Research: Biogeosciences, Vol. 118, pages 1200-1207, doi:10.1002/jgrg.20092

MacIntyre S., Jonsson A., Jansson M., Aberg J., Turney E. T., and Miller D. S. (2010), Buoyancy flux, turbulence, and the gas transfer coefficient in a stratified lake, Geophysical research letters, Vol. 37, L24604, doi:10.1029/2010GL044164, pages 1-5

Sun D., and Lindzen S. R. (1993), Distribution of Tropical Tropospheric Water Vapor, Journal of the Atmospherical Sciences, Vol. 50, No. 12, pages 1643 - 1660

Tranvik L. J., et al. (2009), Lakes and reservoirs as regulators of carbon cycling and climate, *Limnol. Oceanogr.*, *54*(6), 2298-2314, doi: 10.4319/lo.2009.54.6_part_2.2298

Vachon D., Prairie Y. T., and Cole J. J. (2010), The relationship between near-surface turbulence and gas transfer velocity in freshwater systems and its implications for floating chamber measurements of gas exchange, Limnol. Oceanogr., Vol. 55, pages 1723–1732.

Wanninkhof R. (1992), Relationship between wind speed and Gas Exchange over the ocean, Journal of Geophysical Research, Vol. 97, pages 7373-7382

Wik M., Crill P.M., Bastviken D., Danielsson Å., and Norbäck E. (2011), Bubbles trapped in arctic lake ice: Potential implications for methane emissions, J. Geophys. Res., 116, G03044, doi: 10.1029/2011JG001761

Wik M., Thornton B. F., Bastviken D., MacIntyre S., Varner R. K., and Crill P. M. (2014), Energy input is primary controller of methane bubbling in subarctic lakes, Geophys. Res. Lett., 41, doi:10.1002/2013GL058510.

Internet Sources:

Campbell Scientific (2014), CSAT3 Three Dimensional Sonic Anemometer Instruction Manual, [url: http://s.campbellsci.com/documents/us/manuals/csat3.pdf], accessed at 2014-06-24

Jefferies M.O., Richter-Menge J., and Overland J.E. (2014) Arctic Report Card 2014, http://www.arctic.noaa.gov/reportcard

SMHI (2014), Skalor för vindhastighet , [url: http://www.smhi.se/kunskapsbanken/meteorologi/skalor-for-vindhastighet-1.252], accessed at 2014-05-19

14 Appendix A

14.1 Chamber flux measurements

Table A-1. Diffusive CH_4 fluxes measured for years 2010, 2011 and 2012. Daily averages calculated excluding min and max measurements on measurement date. Negative fluxes, measured by chamber i6s on July 4th 2011 and by chamber i2s on August 24th 2011, were considered anomalies and left out of calculation of daily averages *Duplicate date, not included in seasonal average

Date	Measured CH_4 fluxes from shielded chambers mg m^{-2} d^{-1}							Average
	i1s	i2s	i3s	i4s	i5s	i6s	i7s	mg m^{-2} d^{-1}
01/07/10	0.06	3.43	18.32	14.16	17.79			11.79
02/07/10	4.09	4.61	0.95	4.07	0.69			3.04
06/07/10	5.86	25.95	8.9	1.59	8.27			7.68
06/07/10*	15.23	17	13.63	13.91				14.57
07/07/10	2.62	2.8	4.72	6.3	10.92			4.61
09/07/10	20.17	3.55	4.88	4.7	5.06			4.88
13/07/10	7.47	5.45	7.33	1.55	12.9			6.75
20/07/10	4.65	4.47	5.09	5.59	4.27			4.74
26/07/10	4.48	4.89	5.15	5.68	5.67			5.24
27/07/10	3.48	8.93	6	9.27	8.17			7.7
28/07/10	3.77	4.25	5.69	7.48	5.98			5.31
29/07/10	6.8	7.62	7.07	2.47	3.82			5.9
02/08/10	8.61	7.3	11.21	38.04	5.04			9.04
05/08/10		4.73	5.92		8.98			5.92
06/08/10	10.32	3.67	3.05	8.09	3.41			5.06
09/08/10	7.11	5.49	4.99	5.55	6.02			5.69
10/08/10	11	10.3	11.94	11.37	12.97			11.44
Season 2010								**6.55**
04/07/11	5.48	6.06	6.15	4.93	6.18		4.13	5.66
16/07/11	3.8	6.03	1.05	4.85	5.54	43.42	4.6	4.96
20/07/11	5.25	6	2.77	4.42	4.02	9.73	83.75	5.88
25/07/11	3.54	6.15	6.3	8.69	7.4	9.37	8.96	7.5
01/08/11	4.26	5.98	7.51	6.44	0.59	5.85	0.44	4.62
10/08/11	6.22	8.99	11.28	11.16	7.41	5.82	3.88	7.92
24/08/11	16.59		2.02	1.78	1.89	2.46	2.7	2.27
28/08/11	3.49	5.54	9.16	9.41	10.43	13.06	8.83	8.68
07/09/11	2	3.86	5.09	7.33	6.76	7.14	6.71	5.91
12/09/11	1.39	2.41	3.71	3.61	12.69	4.13	5.01	3.78
Season 2011								**5.72**
31/05/12	0.79	1.48	1.76	1.09	1.62	0.88	0.97	1.21
27/06/12	7.61	7.32	7.86		3.52	3.22	3.46	5.48
07/07/12	7.07	7.19	7.45	7.83	5.07	0.56	2.88	5.93
12/07/12	7.95	11.43	17.83	20.45	17.6	17.15	15.38	15.88
20/07/12	14.14	17.38	16.14	14.41	11.54	9.32	6.65	13.11
25/07/12	8.17	9.18	8.95	7.26	6.51	4.73	2.51	7.12
31/07/12	3.43	4.29	5.53	6.37	7.32	7.2	6.73	6.02
08/08/12	5.59	6.46	6.72	7.18	6.21	5.16	3.52	6.03
14/08/12	2.21	2.64	3.59	2.71	2.66	1.99	2.21	2.49
20/08/12	5.61	7.77	6.71	5.53	4.84	4.58	3.17	5.45
29/08/12	2.33	3.24	3.02		2.03	2.05		2.47
04/09/12	2.08	2.02	2.48	2.81	2.72	2.5	2.46	2.45
14/09/12	1	0.94	0.78	2.11	0.67	0.68	1.01	0.88
20/09/12	0.76	0.82	0.73	0.64	0.58	0.52	0.36	0.65
Season 2012								**5.37**

14.2 k_{600} charts – August 4th to August 10th 2010

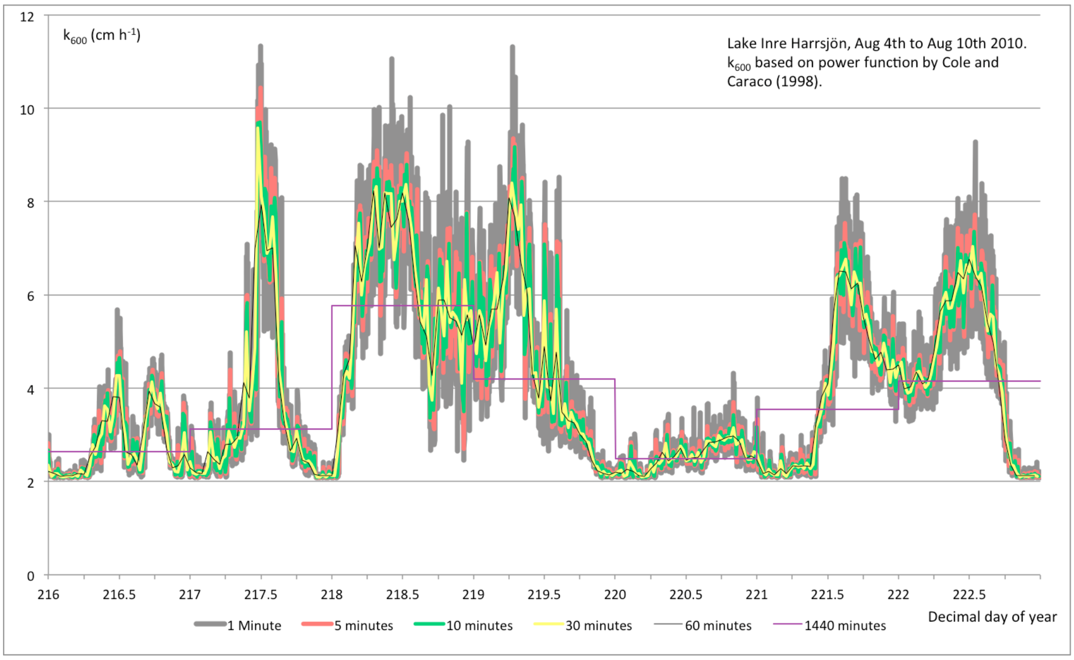

Figure A-1. k_{600} established using power function as described by Cole and Caraco (1998).

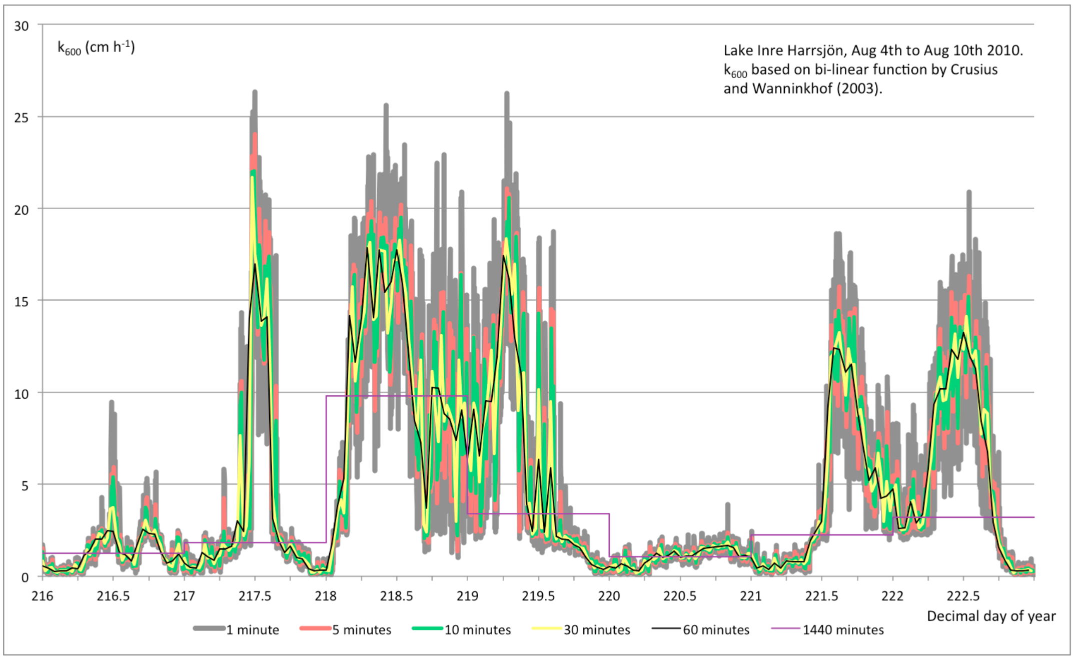

Figure A-2. k_{600} established using bi-linear function as described by Crusius and Wanninkhof (2003).

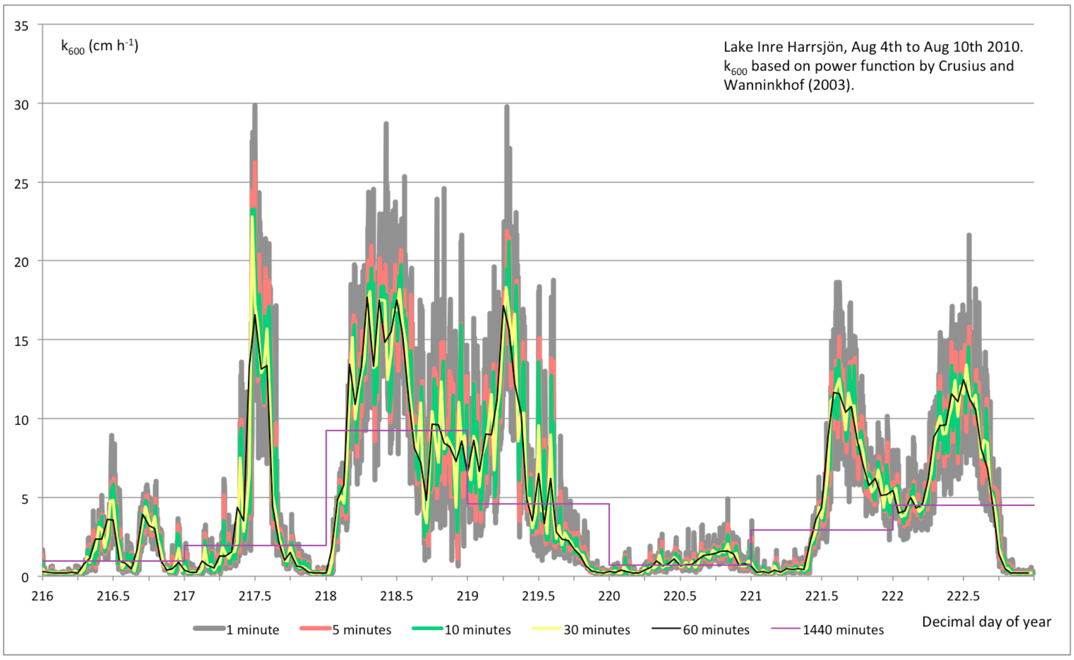

Figure A-3. k_{600} established using power function as described by Crusius and Wanninkhof (2003).

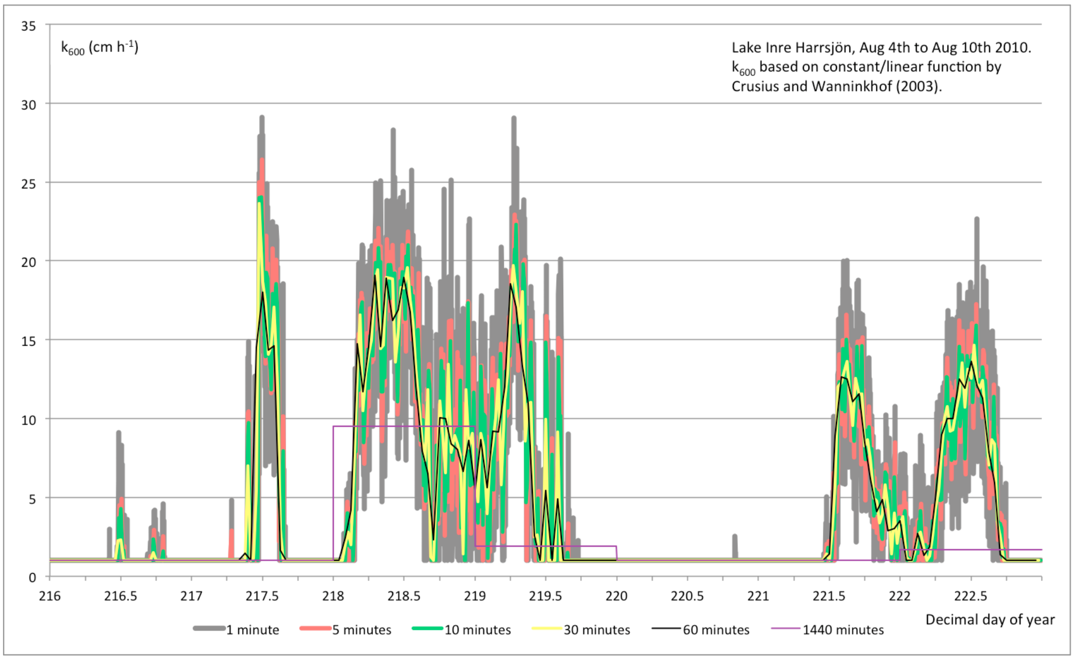

Figure A-4. k_{600} established using constant/linear function as described by Crusius and Wanninkhof (2003).

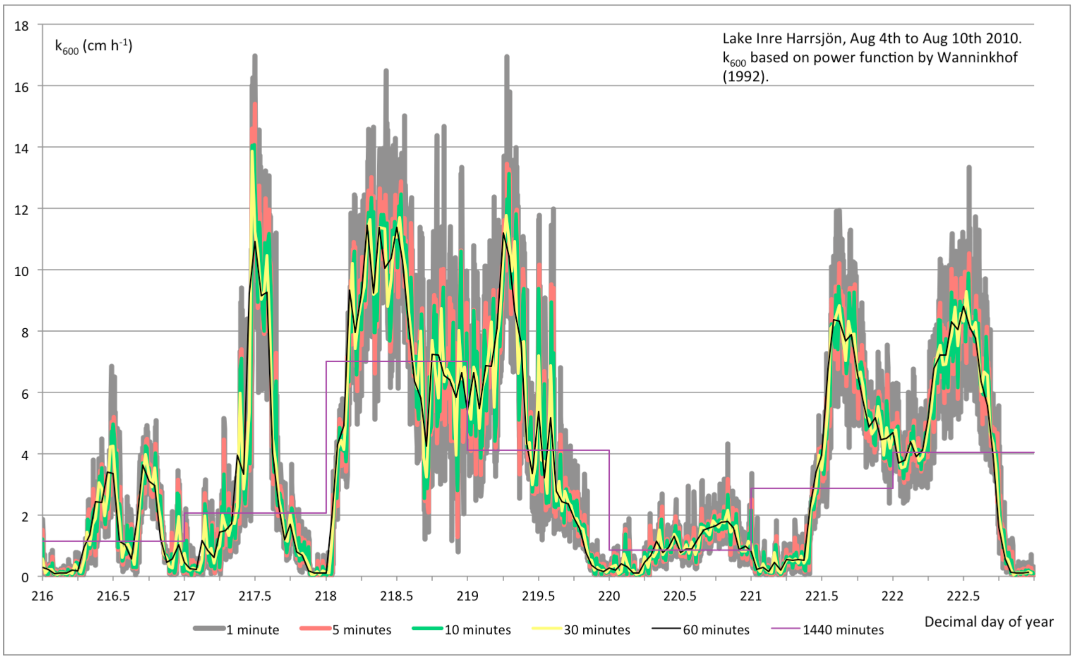

Figure A-5. k_{600} established using power function as described by Wanninkhof (1992).

14.3 k_{600} charts – July 22nd to July 28th 2011

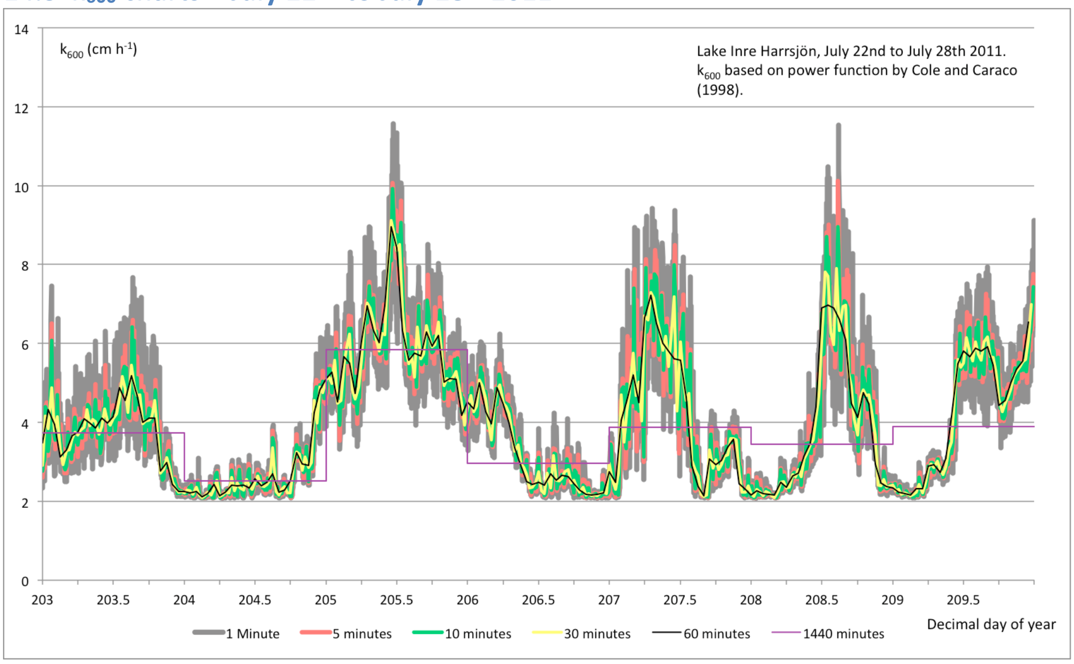

Figure A-6. k_{600} established using power function as described by Cole and Caraco (1998).

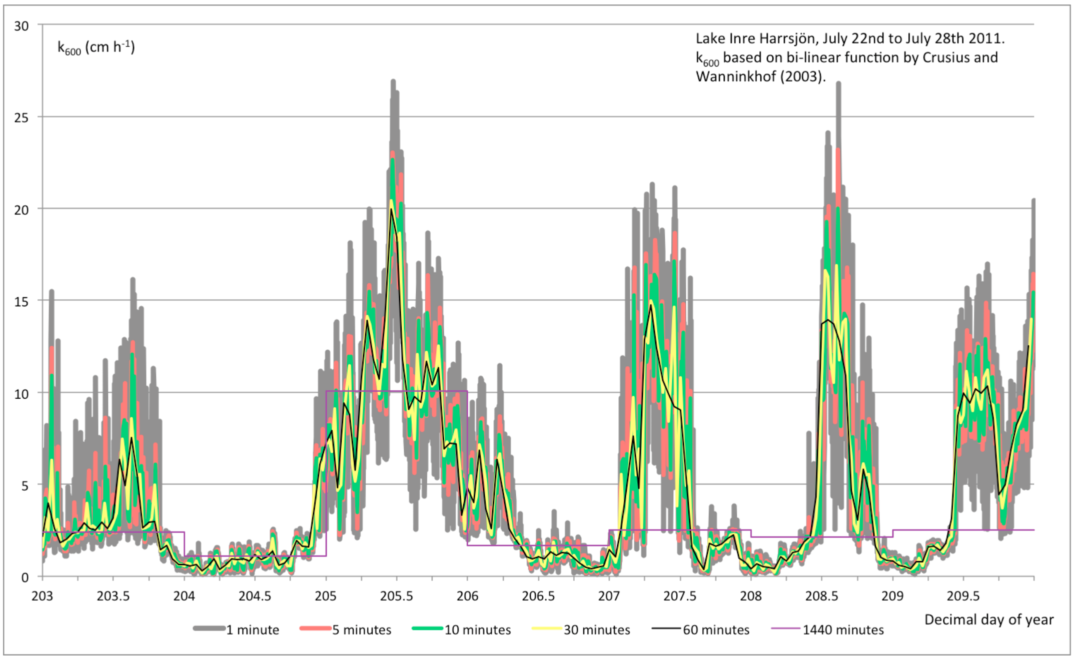

Figure A-7. k_{600} established using bi-linear function as described by Crusius and Wanninkhof (2003).

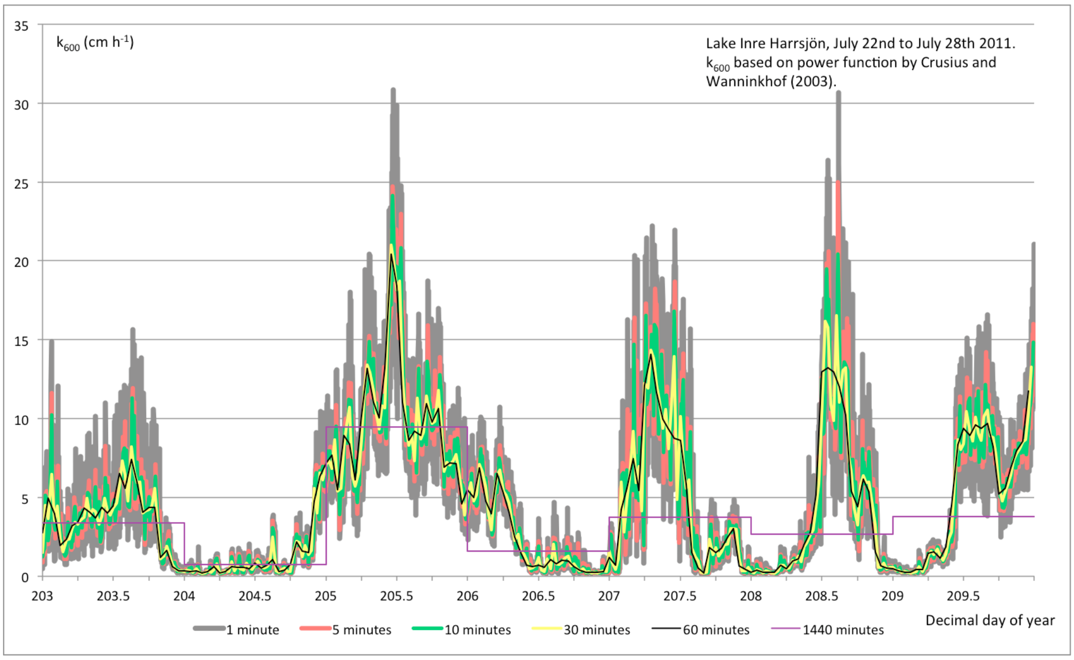

Figure A-8. k_{600} established using power function as described by Crusius and Wanninkhof (2003).

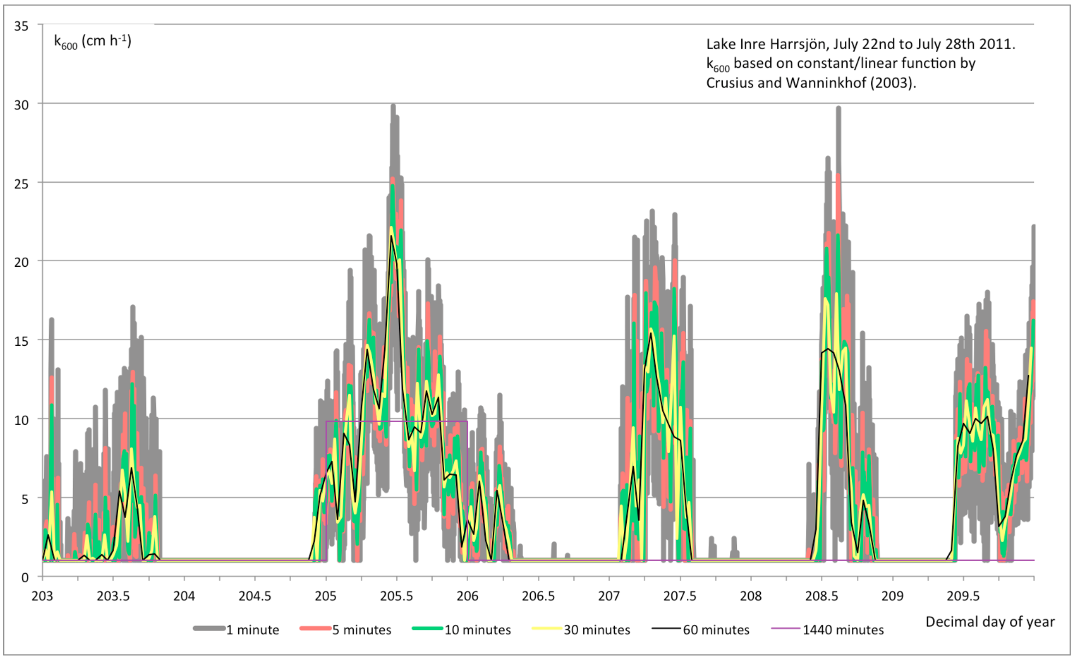

Figure A-9. k_{600} established using constant/linear function as described by Crusius and Wanninkhof (2003).

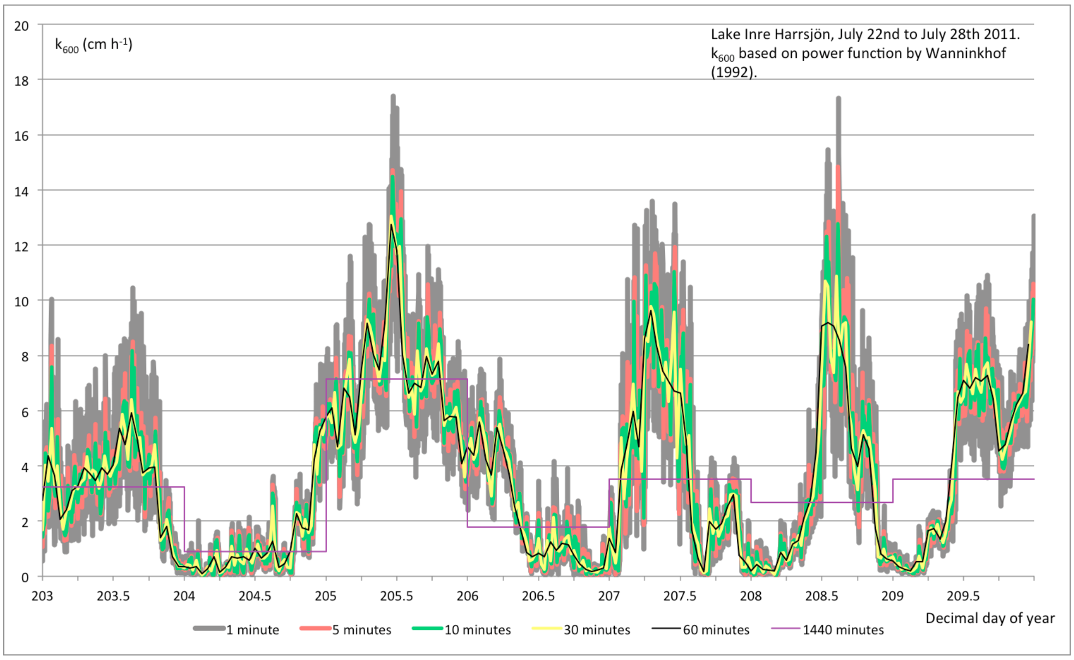

Figure A-10. k_{600} established using power function as described by Wanninkhof (1992).

15 Appendix B

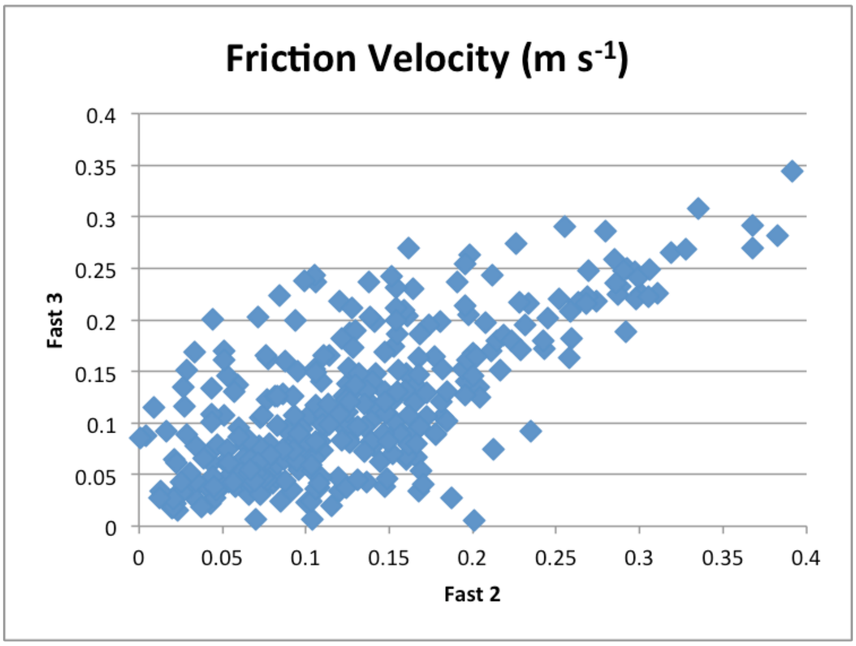

Figure B-1. Friction velocity (u*) for period August 4th to August 10th, 2010, at Inre Harrsjön. Fast 2 and Fast 3 are high frequency (20 Hz) sonic anemometers mounted at same tower, separated by ~ 1 m. Points in plot represent 30 minutes averaging window.

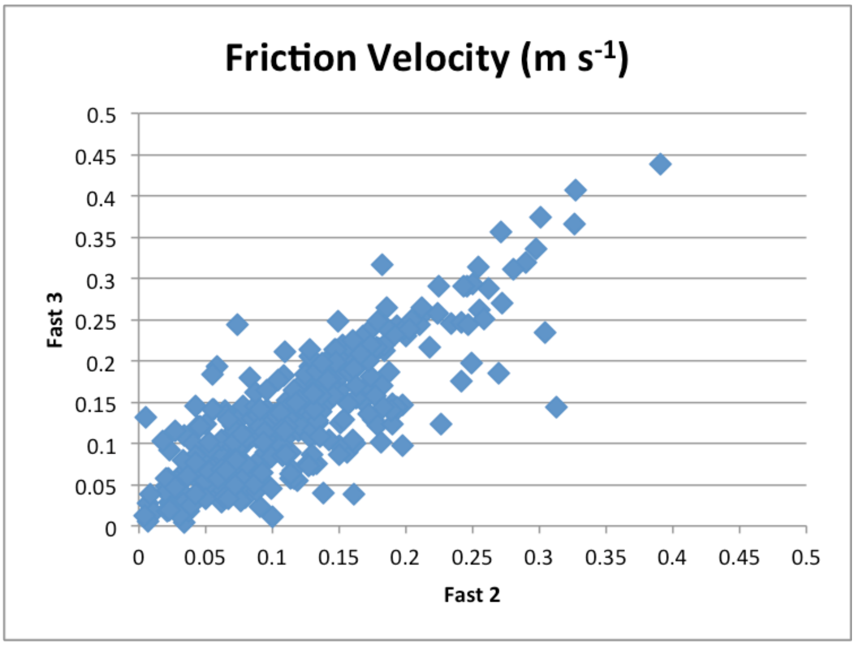

Figure B-2. Friction velocity (u*) for period July 22nd to July 28th, 2011, at Inre Harrsjön. Fast 2 and Fast 3 are high frequency (20 Hz) sonic anemometers mounted at same tower, separated by ~ 1 m. Points in plot represent 30 minutes averaging window.

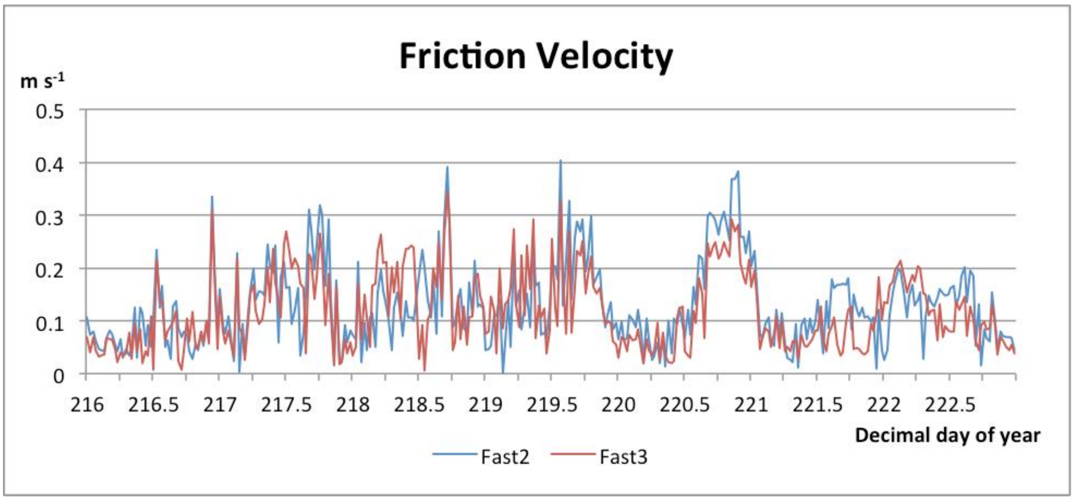

Figure B-3. Friction velocity (u*) for period August 4th to August 10th, 2010, at Inre Harrsjön. Fast 2 and Fast 3 are high frequency (20 Hz) sonic anemometers mounted at same tower, separated by ~ 1 m. Friction velocity calculated at 30 minutes resolution.

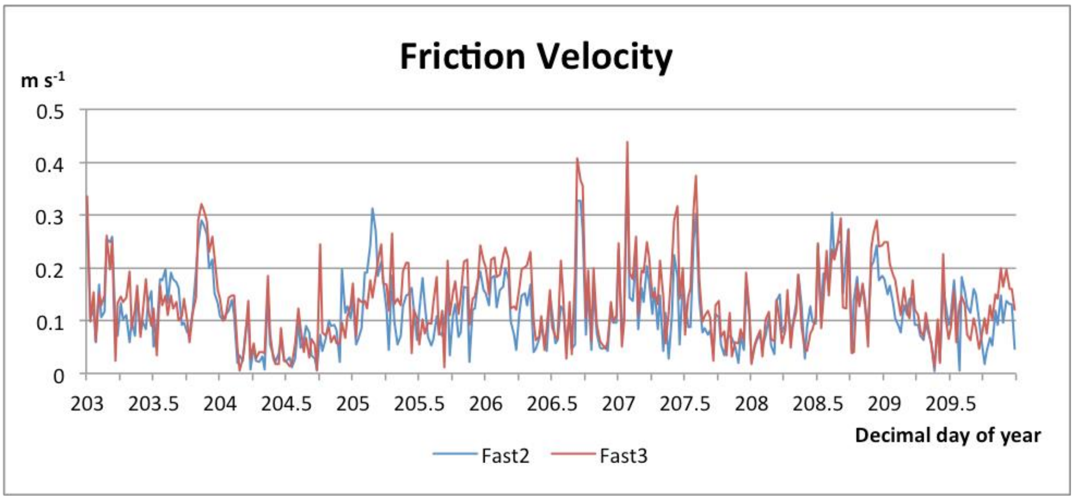

Figure B-4. Friction velocity (u*) for period July 22nd to July 28th, 2011, at Inre Harrsjön. Fast 2 and Fast 3 are high frequency (20 Hz) sonic anemometers mounted at same tower, separated by ~ 1 m. Friction velocity calculated at 30 minutes resolution.